A BOUNDARY-LAYER MODEL FOR BALANCED ARCS

by

Martin D. Cowley

Fluid Mechanics Laboratory

Department of Mechanical Engineering
Massachusetts Institute of Technology

This research has been supported by NASA through grant NGR-22-009-052.

July 1967

A BOUNDARY-LAYER MODEL FOR BALANCED ARCS

Martin D. Cowley

Department of Mechanical Engineering
Massachusetts Institute of Technology, Cambridge, Massachusetts

ABSTRACT

The report discusses two-dimensional arcs which are held stationary against the drag of a stream of gas by the force due to an imposed, transverse, magnetic field. In the proposed model, the arc column is a region which is by-passed by the external stream, but which contains an internal circulatory flow. The effective Reynolds number of the circulation is high enough to justify, as a possible and interesting limit, an analysis in which the action of viscosity and heat conduction are assumed to be confined to thin layers. Gas is supposed to drift forward slowly in an inviscid core of the arc and to be returned rapidly in thin shear layers at the edges. An important consequence is that the state of the gas must be constant along a field line in the core, and the model would be invalid if any field lines are closed within the column.

A solution is found to the equations governing the shear layers in the vicinity of the forward stagnation point of the arc. The velocity profile is peaked, having a ratio of maximum velocity to local value of the external flow approximately equal to one half the square root of the density ratio across the layer. It is shown that, in the subsequent development beyond the stagnation point, the temperature of the gas within the layer may rise above the core value, and flow reversal will be associated with this temperature over-shoot. It is suggested that the phenomenon marks the start of separation of inner and outer flow.

A qualitative discussion suggests that the action of electromotive forces induced by the flow reduces velocity levels in the shear layers and thickens them, while longitudinal flows, predominantly from cathode to anode, are caused by the Hall effect. The theory is not sufficiently developed to predict overall arc behaviour closely, but some similarity conditions can be found, and order-of-magnitude estimates made of size and external flow velocity for a range of values of current and imposed field.

PREFACE

This theoretical study was undertaken during the period of sabbatical leave spent by the author at the Massachusetts Institute of Technology. The report marks the end of the period, and, although the theory has not reached a satisfactory state of completion, time prevents the author from further work. Perhaps a stage has been reached where some experimental confirmation will do more good than any amount of analysis.

Arcs form a complex topic, and it is only the belief that the behaviour of some balanced arcs can be dominated by fluid-mechanic effects that has given the author, who is inexperienced in electrode phenomena, the courage to embark on the study. A tribute should be paid to Professor J. A. Fay and Dr. M. Goldstein; many of the ideas evolved from co-operative efforts during discussions with them. Fay was the first to point out that external and internal pressure distributions could be matched at the stagnation point of an arc and contributed particularly to the ideas on core behaviour. The comments of Professor D. Hoult added stimulation, and his interest in buoyant plumes influenced the theory because of an analogy between magnetic forces in arcs and buoyancy forces.

TABLE OF CONTENTS

LIST OF FIGURES

LIST OF SYMBOLS

a	point of intersection of arc boundary and field line, Section 2.2
	adjustable constant, Eq. (51)
b	point of intersection of arc boundary and field line, Section 2.2
f_0	stream function in the stagnation-point shear layer, Eq. (41)
g	function relating f_0 to h_0, Eq. (48)
h	enthalpy
$\vec{j}$	current density
$\vec{j}_H$	components of current density in the plane of variation caused by the Hall effect
k	quantity controlling the decay of variations at the edge of the shear layers, Section 4.2
	Boltzmann's constant
$\vec{\ell}$	length vector along contour
m'	field-line radius (non-dimensional)
$\vec{n}$	normal vector
n_e	number density of electrons
p	pressure
p_e	pressure of electrons
$\dot{q}$	radiation loss per unit volume
t	time
u	velocity along shear layers
u_∞	free stream velocity
u^0	characteristic velocity, Eqs. (2) and (15)
$\vec{v}$	velocity vector
$\vec{v}_H$	velocity along column induced by the Hall effect

v	velocity transverse to shear layers
x, y	co-ordinates along and transverse to the shear layers with origin at the stagnation point
x^*, y^*	co-ordinates with origin at the center of a circular arc, Section 2.5
x'_e	point of entry to shear layer
z	co-ordinate directed along the arc column
A	z-component of the vector potential of the magnetic field, Section 2.5
$\vec{B}$	magnetic field vector
$\vec{B}_0$	imposed magnetic field
C_D	drag coefficient
$\vec{E}$	electric field vector
$\vec{E}_H$	components of the electric field in the plane of variation caused by the Hall effect
G	Grasshof number, Eqs. (5) and (15)
H	Hall-effect parameter, Eqs. (75)
I	total current
M	induced-emf parameter, Eqs. (75)
N	Alfvén number, Eq. (33)
P	Prandtl number
R	radius of the arc boundary at the stagnation point
R_B	radius of the field line at the stagnation point
S	area between field lines in the core
T	temperature
F	particular solution for f_0, Eq. (47)
H	particular solution for h_0, Eq. (47)

α energy parameter, Eqs. (15)

β parameter controlling the scale of the shear layer, Eq. (53)

γ ratio of number of electrons to total number of particles

δ shear-layer thickness

ε scaling factor, Eqs. (48)

η viscosity

θ angle

μ_0 permeability

ξ shear-layer co-ordinate scaled for density variation, Eq. (41)

ρ density

σ electrical conductivity

τ shear stress

ϕ angle, Section 2.5

unknown function of x, Section 4.2

ϕ_n normal magnetic flux

ψ unknown function of x

Γ circulation

SUPERSCRIPTS

0 reference value of property, taken at the stagnation-point state in the core

on u denotes characteristic velocity, Eqs. (2) and (15)

' quantity non-dimensionalized with respect to reference values of properties, the characteristic velocity, and the nose radius of the arc, Eqs. (15)

* co-ordinates with origin at the arc center, Section 2.5

quantities taken from previous step in iterative solution, Section 3.3

part of linear solution for v_H, Section 5.3

** part of linear solution for v_H, Section 5.3

SUBSCRIPTS

0, 1, 2 terms in shear-layer series, Eqs. (35)

c core value

∞ free stream value

I. INTRODUCTION

Figure 1 shows a cross-section to illustrate what is meant by a balanced arc. The luminous column of ionized gas, where the current flows, is held stationary against a transverse stream by magnetic forces. We assume that the section of arc under consideration is far enough from the electrodes for the flow and magnetic field patterns to be regarded as two-dimensional. For a start, we neglect flow along the column although it will be shown in Section V that the Hall effect can cause such flow. With the assumption of two-dimensionality, a magnetic field $\vec{B}_0$ must be imposed by external coils to cause a net force on the column. Uniform $\vec{B}_0$ gives the simplest circumstances, and then the total force is IB_0 per unit length. This must be balanced by the loss of momentum of the stream, or aerodynamic drag. Another overall condition is that the total electromagnetic energy supplied must equal the loss due to radiation and convection by the stream.

The hypothesis of Lord[1] that the aerodynamic drag is approximately the same as that of a solid cylinder having the same dimensions as the arc suggests that most of the stream is diverted round the column, and a relatively stagnant wake is formed behind. The hypothesis has had some experimental verification in cases where arc dimensions have been measured (for a review see Myers and Roman[2]). With this success, a not surprising conjecture is that at least a major part of the column is a region of closed streamlines, impervious to the outer flow (see, for example, Kuethe et al.[3]). The recent experiments of Roman and Myers[4] on arcs in a

cross flow of air support this view with results of investigations by pitot traverse behind the column, which indicate a stagnant wake, and by injection of particles upstream, which showed no tendency to enter the column, being apparently swept round and shed in vortices similar to those found at the edges of conventional wakes.

The object of the present investigation is to explore the detailed fluid-mechanic behaviour in and near the column on the assumption that the arc is impervious, i.e., there is a forward stagnation point. The suggested model for the flow pattern is broadly that a double vortex forms in a large part of the interior (see Fig. 2a). (The discussion of flow reversal in Section IV, however, suggests that in detail more than two distinct vortices could be formed.) The mechanisms which could drive the motion are two. First is the shearing action of the external stream, which we shall find to be the less important. The second is the rotational nature of the magnetic forces. Suppose that we neglect the electro-motive forces generated by the motion and the Hall effect. Then the magnetic forces tend to change the circulation round the loop ABCDA of Fig. 2a according to

$$\frac{d\Gamma}{dt} = \oint \vec{j} \times \vec{B} \cdot d\vec{\ell}/\rho$$

$$= \oint (\sigma/\rho)\, \vec{E} \times \vec{B} \cdot d\vec{\ell}$$

$$= E \oint (\sigma/\rho)\, \vec{B} \cdot d\vec{n}$$

$$\frac{d\Gamma}{dt} = E \oint (\sigma/\rho)\, d\phi_n \quad , \tag{1}$$

where ϕ_n is the outward normal flux per unit length of the column at the loop, and, in deriving Eq. (1) we have used the fact that $\vec{E}$, being perpendicular to the plane of variation, must be uniform for curl $\vec{E} = 0$.

We expect the mean level of σ/ρ to be very much lower on the cold leg of the loop ABC than on the hot leg CDA. Then with an imposed, transverse field so that we have $\int_A^C d\phi_n \neq 0$, there results a mechanism for inducing circulation. The action of the magnetic forces, which are temperature dependent through σ, has an analogy with that of buoyancy forces in natural-convection problems - an analogy noted also by Kuethe et al.[3] and one which we shall pursue further. A field line corresponds to a line of constant height so that variation of σ along a field line gives a rotational force (see Fig. 2b).

For a steady state the tendency of the magnetic force to increase circulation must be balanced by suppression due to viscous damping.

A characteristic velocity u^0 for the circulation is found by relating the time scale in Eq. (1) to R/u^0, where we take the nose radius R to be typical of arc dimensions, and by relating Γ to $u^0 R$. Thus

$$u^0 = \sqrt{(\sigma^0 \, EB^0 \, R/\rho^0)} \quad , \tag{2}$$

where the superscript 0 on the quantities σ, B, ρ, also refers to characteristic values for the interior flow. This velocity can be related to that of the free stream by defining the drag coefficient as

$$C_D = (\pi\sigma^0 \, EB^0 \, R)/(\rho_\infty u_\infty^2) = O(1) \quad . \tag{3}$$

Then

$$u^0 = u_\infty \sqrt{\{(C_D \rho_\infty)/(2\rho^0 \pi)\}} \ , \tag{4}$$

which suggests that the rotational effect of the magnetic forces is larger than that of the shearing action of the free stream by a factor of order $\sqrt{(\rho_\infty/\rho^0)}$.

The square of the Reynolds number based on the characteristic velocity is

$$G = \rho^0 \, \sigma^0 \, E \, B^0 R^3/\eta^{0^2} \ . \tag{5}$$

Following Kuethe et al.[3], we call this quantity the Grasshof number, since it has the same significance as the Grasshof number in natural-convection problems. Relating G to the Reynolds number based on free-stream properties and velocity by means of Eq. (3), we obtain

$$G = (C_D/\pi) \, (\rho^0/\rho_\infty) \, (\eta_\infty/\eta^0)^2 \, Re_\infty^2 \ . \tag{6}$$

The quantity $(\rho^0/\rho_\infty)(\eta_\infty/\eta^0)^2$, which appears in Eq. (6), is plotted in Fig. 3 for air assuming atmospheric pressure, a free-stream temperature of $300^\circ K$, and thermodynamic equilibrium (property values were taken from the report of Arave et al.[5]). A reasonably representative value of G is then $10^{-4} \, Re^2$ (assuming $C_D = 0(1)$). The experiments of Roman and Myers[4], for

which size of arc and blowing velocity are well documented, gave a range for Re from 10^3 to 10^4, i.e., $G \simeq 10^2 - 10^4$.

The values of G given above suggest that there can be at least a range of arc conditions for which inertia effects in the column are strong (recall $G^{1/2}$ is the effective Reynolds number for circulation). Now in problems of natural convection $G^{1/4}$ is the scaling for boundary-layer thickness (see, for example the boundary layer on a heated vertical plate). With large values of $G^{1/4}$ it is possible that a successful model of the arc can be found in which viscous effects are confined to thin layers, and the following theory represents a start on such a model. However, the experimental range of Roman and Myers[4] did not extend to high enough values, and the analysis will be a limit, hopefully to be approached by known arcs.

II. APPROXIMATIONS

2.1 THE MODEL

Fig. 4 illustrates our model for the forward part of the arc column. We suppose that the action of viscosity and heat conduction is negligible except in thin shear layers at the edge. The gas moves forward in an inviscid core, and, being entrained by the shear layers, is swept back in them. Note that the supposed entrainment provides a mechanism to counteract viscous diffusion. The validity of the model rests with our being able to find a solution which satisfactorily matches the outer inviscid flow to the inner and then to show that assumptions about the action of diffusion processes were valid. It is possible to give some justification by considering the expected orders of magnitude.

Again we assume that the nose radius R is typical of arc dimensions, both parallel and transverse to the free stream. The fact that $C_D = O(1)$

suggests that pressure gradients are of order $\sigma^0 EB^0$. When a fluid particle enters the shear layers, it may be cooled to a temperature at which it is virtually non-conducting, while still being hot enough to have a density comparable to the core. Thus, in being swept back, the particle experiences little magnetic force, but can fall through a pressure difference $O(\sigma^0 EB^0 R)$, and, according to Eq. (2), it can thereby attain a speed of the order of the characteristic velocity u^0. Note that, by reason of continuity, the core velocity will be $O(u^0\delta/R)$, where δ is the shear-layer thickness, and exterior velocities will be $O\{u^0\sqrt{(\rho^0/\rho_\infty)}\}$, i.e., the velocity profile is peaked. Viscous shear stress in the layers will be $O(\eta^0 u^0/\delta^2)$, and, assuming viscous forces comparable to inertia forces, we obtain the expected result for thickness:

$$\delta/R = \sqrt{\{\eta^0/(\rho^0 u^0 R)\}} = G^{-1/4} \quad . \tag{7}$$

We are suggesting that the shear layers are regions where pressure, inertia, magnetic and viscous forces are all comparable. However, the low velocity in the core implies that both inertia and viscous forces are negligible there in comparison to magnetic (being $O(G^{-1/2})$), and there must be a balance between pressure and magnetic forces only.

As in conventional boundary and shear layers, continuity gives a transverse velocity $O(u^0 G^{-1/4})$; viscous stresses would require pressure differences across the layer only of order $G^{-1/2}$. However, since the magnetic force may have a large component perpendicular to the layer, transverse magnetic forces can cause a pressure difference $O(G^{-1/4})$ - the

vicinity of the stagnation point needs special consideration (see Section 2.4). Also accelerations due to curvature require pressure differences $O(G^{-1/4})$, and it is only to this low order of approximation that we can take pressure to be continuous across the layer.

We now turn to the energetic aspects of the model. In the same way that the entrainment provides a mechanism to counteract viscous diffusion of the layers, it will also counteract thermal diffusion, and for Prandtl number $P = O(1)$ we expect the scale for thermal and viscous layers to be the same. (An additional reason for assuming the same scale is the coupling between energy and momentum through the temperature-dependent forces. Thus for $P \to 0$, the velocity scale is determined by thermal diffusion.) Gradients of enthalpy across the layer are $O(h^0/\delta)$, and it is assumed that the enthalpy difference between the rear of the column and the forward stagnation point is $O(h^0)$, so that gradients in the core are $O(h^0/R)$. Supposing that radiation does not absorb a major part of the power input, the heat loss across the layer $O(\eta^0 h^0 R/P\delta)$ has to be comparable to the power input to the whole arc $O(\sigma^0 E^2 R^2)$. From the small area of the layers it follows that in comparison to both conduction and convection terms the electromagnetic power in the layer is $O(G^{-1/4})$ and may be neglected to a low order of approximation. In the core, convection is reduced by $G^{1/4}$ since the velocity is $O(u^0 G^{-1/4})$, so that convection and power input can balance, while conduction is reduced by $G^{1/2}$, i.e. compared to convection, conduction is $O(G^{-1/4})$ in the core and may be neglected to a low order of approximation.

Aspects which we leave for later consideration are the electromotive forces and the Hall effect.

2.2 CORE EQUATIONS AND BEHAVIOUR

According to the order-of-magnitude considerations of the last section, the force balance in the core requires (neglecting terms $O(G^{-1/4})$)

$$\text{grad } p = \vec{j} \times \vec{B} = \sigma \vec{E} \times \vec{B} \quad , \tag{8}$$

and there can be no pressure variation along a field line. The distance between adjacent lines is inversely proportional to B, so that grad p varies like B along a field line. Since $\vec{E}$ is uniform and perpendicular to $\vec{B}$, it follows that Eq. (8) can only be satisfied if σ as well as p is constant along any field line, i.e., the state of the gas does not vary in the direction of $\vec{B}$.

A departure of order only $G^{-1/4}$ from the balance of Eq. (8) is capable of giving any velocity changes required in the core, but a condition is imposed by the energy equation for a fluid particle:

$$\rho \frac{dh}{dt} = \sigma E^2 - \dot{q} \quad , \tag{9}$$

where $\dot{q}$ represents the radiation, and we assume that there is negligible absorption so that $\dot{q}$ is a function of the local state only. Hence dh/dt is constant on any one field line, and, since dh is the same for all fluid particles as they travel between adjacent lines, it follows that the time of flight dt is the same. Then the velocity component normal to a field line varies like 1/B along it. A geometric illustration of the above arguments is given in Fig. 5a.

To determine the magnitude of the velocity component normal to the magnetic field, we use the continuity condition and equate the total mass flow crossing any field line in the core between the points where it intersects the boundaries (ab of Fig. 5b) to the mass flow back in the shear layers. (The velocity component parallel to the magnetic field can be derived from the continuity equation, but we have found no simple, yet general, relation for this component.)

Assuming the arc to be symmetric about an axis through the forward stagnation point and parallel to the free stream, we shall consider the overall energy and continuity for one side of this axis. Suppose δS to be the area between two adjacent field lines (shown cross-hatched in Fig. 5b). The power input less radiation is $(\sigma E^2 - \dot{q})\,\delta S$ to this area. Let x denote a co-ordinate measured along a shear layer with origin at the stagnation point. Then, from the order-of-magnitude arguments of Section 2.1, we expect entrainment velocities $O(u^0 G^{-1/4})$ and, to anticipate the shear-layer definitions of Section 2.4, we define the entrainment at any point as $\rho^0 u^0 G^{-1/4}(\rho_c' v_c')$, where $\rho_c' v_c'$ is a positive number with magnitude O(1). The mass flow crossing the shaded area is thus $\rho^0 u^0 G^{-1/4} \int_0^x \rho_c' v_c'\, dx$, and an overall energy balance gives

$$\frac{\partial h}{\partial x} = \frac{(\sigma E^2 - \dot{q})}{\rho^0 u^0\, G^{-1/4} \int_0^x \rho_c' v_c'\, dx} \frac{\partial S}{\partial x} \quad . \tag{10}$$

We have derived necessary conditions on the velocity profiles and variation of state on the hypothesis of an inviscid, convection-dominated core. It is not obvious that there are causal mechanisms for the formation of the flow pattern. If it could be shown that the flow is stable in the

presence of small disturbances, we might have more confidence. A stability analysis is not attempted here, but it is worth recording the following physical arguments. If the gas state were to become non-uniform along a field line, the magnetic forces induce a circulation which increases the forward velocity of the hotter particles. Then the time of flight for these particles between adjacent field lines becomes less than that of the cold, an effect which tends to reduce their enthalpy increase with distance, or to equalize the state on field lines again. It should be pointed out that this mechanism could be offset by the increase in power input associated directly with the higher electrical conductivity of the hotter particles.

2.3 PRESSURE MATCH AT THE STAGNATION POINT

With symmetry about an axis parallel to the free stream, the magnetic field is parallel and magnetic forces transverse to the shear layer at the stagnation point. It is the curvature of the arc boundary which allows the pressure variation of core and outer flow to be matched there.

Fig. 6a shows the vicinity of the forward stagnation point with shear-layer thickness represented as negligible. Suppose the field line passing through the stagnation point has radius of curvature R_B. Then the angle between the field line and the shear layer at a small distance x from the stagnation point is given by

$$x\left(\frac{1}{R} + \frac{1}{R_B}\right) \quad .$$

For the component of the magnetic force along the shear layer, we can take the magnitudes of σ_c EB as constant to a first approximation, so that the pressure gradient in the core is directly proportional to x:

$$\frac{\partial p}{\partial x} = - \sigma_c \, E \, B \, x \, (\frac{1}{R} + \frac{1}{R_B}) \quad . \tag{11}$$

A linear variation of this type is characteristic of the flow at the stagnation point of a blunt body, so that matching is possible.

Another way of making the same point is illustrated in Fig. 6b, which shows isobars in the core for the case of uniform field, $R_B \to \infty$. If the distance from the stagnation point to an isobar is x along the boundary, the perpendicular distance is $x^2/2R$, i.e., the difference in pressure from that at the stagnation point varies like x^2 along the boundary.

2.4 SHEAR-LAYER EQUATIONS

In writing equations for the shear layers we assume that they are thin enough in comparison to their radius for the effects of curvature to be negligible (which implies that the approximation is valid only to zero order in $G^{-1/4}$). Taking the co-ordinate system of Fig. 4 with the x-direction along the layer and y-direction transverse and outward, the usual boundary-layer approximations yield the following equations for continuity, longitudinal momentum and energy:

$$\frac{\partial(\rho u)}{\partial x} + \frac{\partial(\rho v)}{\partial y} = 0 \quad , \tag{12}$$

$$\rho u \frac{\partial u}{\partial x} + \rho v \frac{\partial u}{\partial y} + \frac{\partial p}{\partial x} = - \sigma \, E B_y + \frac{\partial}{\partial y} (\eta \frac{\partial u}{\partial y}) \quad , \tag{13}$$

$$\rho u \frac{\partial h}{\partial x} + \rho v \frac{\partial h}{\partial y} = \{\sigma E^2\} + \frac{\partial}{\partial y} (\frac{\eta}{P} \frac{\partial h}{\partial y}) \quad , \tag{14}$$

where we have retained the term in braces of Eq. (14) since its effect is unfamiliar although, according to the arguments of Section 2.1, we expect it to be $O(G^{-1/4})$.

Suppose that characteristic values of the thermodynamic properties, ρ^0, h^0, etc., are those of the core at the stagnation point. We take B^0 as the value of the applied field there and non-dimensionalize the equations in accordance with the order of magnitudes suggested in Section 2.1:

$$\rho' = \rho/\rho^0 \quad , \quad h' = h/h^0 \quad , \quad \sigma' = \sigma/\sigma^0 \quad , \quad B_y' = B_y/B^0 \quad ,$$

$$\eta' = \eta/\eta^0 \quad , \quad \dot{q}' = \dot{q}/\sigma^0 E^2 \quad , \quad p' = (p - p^0)/\rho^0 u^{0^2} \quad ,$$

$$u' = u/u^0 \quad , \quad v' = (v/u^0)\, G^{+1/4} \quad ,$$

$$x' = x/R \quad , \quad y' = (y/R)\, G^{+1/4} \quad , \tag{15}$$

$$\alpha = (\sigma^0 E^2 R/\rho^0 u^0 h^0)\, G^{+1/4} \quad , \quad u^0 = (\sigma^0 E B^0 R/\rho^0)^{1/2} \quad ,$$

$$G = \rho^0 \sigma^0 E B^0 R^3/\eta^{0^2} \quad .$$

For ease of reference we have repeated the definitions of u^0 and G. Substitution from Eqs. (15) and Eqs. (12), (13) and (14) gives

$$\frac{\partial(\rho' u')}{\partial x'} + \frac{\partial(\rho' v')}{\partial y'} = 0 \quad , \tag{16}$$

$$\rho' u' \frac{\partial u'}{\partial x'} + \rho' v' \frac{\partial u'}{\partial y'} + \frac{\partial p'}{\partial x'} = - \sigma' B_y' + \frac{\partial}{\partial y'} \left(\eta' \frac{\partial u'}{\partial y'} \right) \quad , \tag{17}$$

$$\rho' u' \frac{\partial h'}{\partial x'} + \rho' v' \frac{\partial h'}{\partial y'} = \{ \alpha G^{-1/4} \} (\sigma' - \dot{q}') + \frac{\partial}{\partial y'} \left(\frac{\eta'}{P} \frac{\partial h'}{\partial y'} \right) \quad . \tag{18}$$

If again we make the usual boundary-layer assumptions in the transverse momentum equation, we have

$$\frac{\partial p'}{\partial y'} = (\sigma' B_x') \, G^{-1/4} \quad , \tag{19}$$

where all terms of order $G^{-1/4}$ are dropped except the unfamiliar magnetic force. Near the stagnation point the angle between field lines and the arc boundary relates B_x' to B_y' by

$$B_y' = x'(1 + 1/R_B') \, B_x' \quad .$$

We will therefore have $\partial p'/\partial y' = O(\partial p'/\partial x')$ over a length given by $x' = O(G^{-1/4})$. However, the stagnation-point solution will be found to be of the usual type with $\sigma' B_x'$ a function of y' only to a first approximation, and it may be shown that departure from $\partial p'/\partial x' = \text{const.}$ across the layer is $O(G^{-1/4})$ even when $x' = O(G^{-1/4})$.

If the magnetic field is non-uniform, we have from the continuity equation for the field

$$\frac{\partial B_y'}{\partial y'} = O(G^{-1/4}) \quad , \tag{20}$$

and to a first approximation B'_y is constant across the layer. Then, since to order $G^{-1/4}$ the magnetic force is balanced by the pressure gradient only in the core, it follows from Eqs. (19), (20) and (17) that

$$\frac{\partial p'}{\partial x'} = - \sigma'_c \, B'_{yc} + O(G^{-1/4}) \quad , \tag{21}$$

where the subscript c refers to the core value at a given x.

We derive boundary conditions on the core side from the facts that

$$u' \to O(G^{-1/4}) \quad , \quad \frac{\partial h'}{\partial y'} \to O(G^{-1/4}) \quad \text{as} \quad y' \to - O(G^{+1/4}) \quad . \tag{22}$$

Therefore we take h' as independent of y' when $y' \to - \infty$, and the variation with x follows from the core analysis of Section 2.2. Non-dimensionalizing Eq. (10), we obtain

$$\frac{\partial h'_c}{\partial x'} = \frac{\alpha(\sigma'_c - q'_c)}{x' \displaystyle\int_0 \rho'_c v'_c \, dx'} \frac{\partial S'}{\partial x'} \quad . \tag{23}$$

On the outer side of the shear layers the usual conditions apply for approach to an inviscid, isothermal flow.

At this point we can note that, provided the field changes moderately throughout the arc, $\partial S'/\partial x'$ is O(1), and Eq. (23) shows α to be O(1) if $\partial h'_c/\partial x'$ is O(1). Then the electromagnetic-power term in Eq. (18) is $O(G^{-1/4})$ and may be dropped.

To complete the description of the shear layers, property relations are needed. It is assumed that the Mach number of the free stream is low enough for pressure differences to be a small fraction of the absolute pressure so that ρ', σ', etc., may be taken as functions of h' only. (Note that a low Mach number is sufficient condition for the neglect of the kinetic energy in the energy equation in spite of the fact that $u^0 = 0\{\sqrt{(\rho_\infty/\rho^0)}\, u_\infty\}$. The high velocities are expected in regions of low density where h^0 characterizes values of enthalpy, and we have $u^{0^2}/h^0 = (u_\infty^2/h_\infty)\,(\rho_\infty h_\infty/\rho^0 h^0)$, where $\rho_\infty h_\infty/\rho^0 h^0 = 0(1)$.)

Then to summarize the complete system of equations and boundary conditions, we have

$$\frac{\partial \rho' u'}{\partial x'} + \frac{\partial \rho' v'}{\partial y'} = 0 \quad , \tag{24}$$

$$\rho' u' \frac{\partial u'}{\partial x'} + \rho' v' \frac{\partial u'}{\partial y'} = (\sigma_c' - \sigma')\, B_{yc}' + \frac{\partial}{\partial y'}\left(\eta' \frac{\partial u'}{\partial y'}\right) \quad , \tag{25}$$

$$\rho' u' \frac{\partial h'}{\partial x'} + \rho' v' \frac{\partial h'}{\partial y'} = \frac{\partial}{\partial y'}\left(\frac{\eta'}{P} \frac{\partial h'}{\partial y'}\right) \quad , \tag{26}$$

$$\rho' = \rho'(h') \quad , \quad \sigma' = \sigma'(h') \quad , \quad \eta' = \eta'(h') \quad , \quad P = P(h') \quad , \tag{27}$$

$$u' \to 0 \quad , \quad h' \to h_c' \quad , \quad \text{as } y' \to -\infty \quad , \tag{28}$$

$$\frac{\partial}{\partial y'}\left(\frac{\partial u'}{\partial x'}\right) \to 0 \quad , \quad h' \to h_\infty' \quad \text{as } y' \to \infty \quad . \tag{29}$$

2.5 ELLIPTIC ASPECTS

Given the free-stream enthalpy and pressure, property relations of the form (27) can be constructed if we assume a value of h'_∞ (which essentially implies a choice of h^0). If we also assume B'_{yc} and $\partial S'/\partial x'$ are known functions of x' and α is a known constant, the parabolic system of equations represented by (23) - (29) can in principle be integrated step by step. We therefore have a family of solutions for the shear layers characterized by the parameters (some functional)

$$(B'_{yc} \ , \ \partial S'/\partial x' \ , \ \alpha \ , \ h'_\infty) \ . \tag{30}$$

These four parameters carry the elliptic aspects of the problem.

The physical significance of the elliptic parameters is as follows. For a particular shape, the magnetic field (and hence both B'_{yc} and $\partial S'/\partial x'$) depends on the current distribution over the whole cross-section of the arc, while the shape itself must be chosen to match the pressure distribution for inner and outer flows along the complete boundary. The significance of α is that, for given field, h^0 and E, it is a function of the nose radius R and is therefore closely connected with arc size. The freedom at present left in the problem by the two unknowns α and h' will disappear if there are two boundary conditions on the shear layers to be applied at the rear of the arc. This point will be discussed further in Section 6, but we can surmise here that the conditions might arise out of a need to close the internal streamlines.

To indicate some features of the self field, we take a highly simplified model in which the arc is a circular cylinder of radius R with uniformly distributed current density j. The latter assumption is equivalent to having uniform core properties; the shear-layer contribution to the self field is $O(G^{-1/4})$. Suppose co-ordinates (x^*, y^*) have their origin at the center of the arc (see Fig. 7a). Then, if A is the z-component of the vector potential, we have in the interior of the arc

$$A = - \{B_0 x^* + 1/4\ \mu_0 j(x^{*2} + y^{*2})\} \quad , \tag{31}$$

where B_0 is the imposed field and assumed to be uniform. With this geometry the self field has no transverse component at the arc boundary, and the magnetic force along the shear layers is the same as for no self field. This explains the choice of the applied-field value in the non-dimensional scheme of Eqs. (15). The result will not be generally true with realistic shapes and current distributions, but there will be a tendency for the self field to have a weak influence on B_y' at the boundary.

Non-dimensionalizing x* and y* with respect to R and rearranging Eq. (31) we obtain

$$\frac{4B_0^2}{\mu_0^2 j^2 R^2} - \frac{4A}{\mu_0 jR} = (x^{*\prime} + \frac{2B_0}{\mu_0 jR})^2 + y^{*\prime 2} \quad , \tag{32}$$

which shows that the field lines in the column (A = const.) are circular arcs centered on the axis of symmetry at a distance $2B_0/\mu_0 jR$ upstream of

the arc center. If $2B_0/\mu_0\, jR < 1$, the field direction at the stagnation point becomes opposite to that of the applied field, and there will be closed field lines within the core. This would clearly be incompatible with the core theory of Section 2.2, so that the boundary-layer model cannot be valid with a field reversal. The parameter $\mu_0\, jR/2B_0$ can be expressed in a more convenient way by using the drag relation (3). Eliminating jR, it becomes

$$N^2 = \frac{C_D}{2\pi} \frac{\mu_0 \rho_\infty u_\infty^2}{B_0^2} \quad , \tag{33}$$

where N is essentially an Alfvén number for the arc.

We can find the area between two field lines by elementary trigonometry (see Fig. 7b) and hence derive $\partial S'/\partial x'$ for Eq. (23). Consider two field lines of non-dimensional radii m' and m' + δm' which intersect the arc boundary at a distance δx' apart. The angles between the axis of symmetry and lines joining the intersection points to the arc center and the field-line center are θ and φ. Then the area δS' is m'φδm'. But $\delta m' = \delta x' \sin(\theta + \phi)$, and $m'/\sin\theta = (2B_0/\mu_0\, jR)/\sin(\theta + \phi) = 1/\sin\phi$. Hence

$$\frac{\partial S'}{\partial x'} = (2B_0/\mu_0\, jR) \sin\theta \tan^{-1} \left\{ \frac{\sin\theta}{(2B_0/\mu_0\, jR) - \cos\theta} \right\} ,$$

$$= (2B_0/\mu_0\, jR) \sin x' \tan^{-1} \frac{x'}{(2B_0/\mu_0 jR) - (1 - x'^2)}$$

$$\to \frac{x'^2}{1 - (\mu_0\, jR/2B_0)} \quad \text{as} \quad x' \to 0 \quad . \tag{34}$$

Note that $\partial S'/\partial x' \to 1/2\pi\ (2B_0/\mu_0\ jR)\ x'$ at the critical condition $2B_0/\mu_0\ jR = 1$, when there is a neutral point in the field at the stagnation point.

III. THE STAGNATION-POINT SHEAR LAYER

3.1 REDUCTION OF EQUATIONS

Section 2.3 showed that the pressure variation along the shear layers is like that on conventional blunt bodies. It is consistent with this result to take the velocity u' as initially varying linearly with x'. It is clear from Eqs. (23) and (34) that the departure of h_c' from the stagnation-point value (unity) has a quadratic dependence on x' initially. Hence we assume that properties can be expanded according to the following power series:

$$
\begin{aligned}
u' &= x'(u_0 + u_1 x'^2 + u_2 x'^4 + \ldots\ldots) \\
v' &= v_0 + v_1 x'^2 + v_2 x'^4 + \ldots\ldots \\
h' &= h_0 + h_1 x'^2 + h_2 x'^4 + \ldots\ldots \\
h_c' &= 1 + h_{1c} x'^2 + h_{2c} x'^4 \ldots\ldots \\
&\qquad\qquad \text{etc.}
\end{aligned}
\tag{35}
$$

With the elementary description of the field given in Section 2.5, the transverse magnetic field at the boundary of the arc is that due to the imposed field only, so that

$$B'_{yc} = \sin x'$$

$$= x' - x'^3/3! + \ldots\ldots \tag{36}$$

When the series (35) and (36) are substituted into the shear-layer equations (23) - (28), and the lowest order terms in x' are equated, we obtain

$$\rho_0 u_0 + \frac{\partial \rho_0 v_0}{\partial y'} = 0 \quad , \tag{37}$$

$$\rho_0 u_0^2 + \rho_0 v_0 \frac{\partial u_0}{\partial y'} = (1 - \sigma_0) + \frac{\partial}{\partial y'} \left(\eta_0 \frac{\partial u_0}{\partial y'}\right) \quad , \tag{38}$$

$$\rho_0 v_0 \frac{\partial h_0}{\partial y'} = \frac{\partial}{\partial y'} \left(\frac{\eta_0}{P} \frac{\partial h_0}{\partial y'}\right) \quad , \tag{39}$$

$$h_{1c} = - \frac{\alpha(1 - \dot{q}_{0c})}{2\rho_0 v_{0c}} \frac{1}{(1 - \mu_0 \, jR/2 \, B_0)} \quad . \tag{40}$$

Now make the usual boundary-layer substitution:

$$\xi = \int \rho_0 \, dy' \quad , \quad f_0 = - \rho_0 v_0 \quad , \tag{41}$$

so that, from Eq. (37),

$$\frac{df_0}{d\xi} = u_0 \quad . \tag{42}$$

Then our system of equations for the shear layers at small x' (i.e., near the stagnation point) becomes

$$\frac{d}{d\xi}\left(\rho_0 \eta_0 \frac{d^2 f_0}{d\xi^2}\right) + f_0 \frac{d^2 f_0}{d\xi^2} = \left(\frac{df_0}{d\xi}\right)^2 - \left(\frac{1 - \sigma_0}{\rho_0}\right) \quad , \tag{43}$$

$$\frac{d}{d\xi}\left(\frac{\rho_0 \eta_0}{P} \frac{dh_0}{d\xi}\right) + f_0 \frac{dh_0}{d\xi} = 0 \quad , \tag{44}$$

with boundary conditions taken from Eqs. (28) and (29):

$$\begin{aligned} &\frac{df_0}{d\xi} \to 0 \quad , \quad h_0 \to 1 \quad \text{as} \quad \xi \to -\infty \quad , \\ &\frac{d^2 f_0}{d\xi^2} \to 0 \quad , \quad h_0 \to h'_\infty \quad \text{as} \quad \xi \to +\infty \quad , \end{aligned} \tag{45}$$

The initial stages of the core development are given by

$$h_{1c} = \frac{(1 - q_{0c})}{2 f_{0c}(1 - \mu_0 \sqrt{R/2}\, B_0)} \quad . \tag{46a}$$

The resemblance of Eqs. (43) and (45) to those governing natural convection on a flat vertical plate is marked. The term $(1 - \sigma_0)/\rho_0$ corresponds to the buoyancy force. (An exact analogy to the incompressible boundary layer can be formed with an arc next to a cold, solid, flat boundary if $(1 - \sigma_0)/\rho_0$ can be taken as a linear function of h_0 and $\rho_0 \eta_0$ as constant, = 1.)

The most significant term in the equations is the 'driving term' $(1 - \sigma_0)/\rho_0$ (recall that this represents the effect of the difference between the pressure gradient and the magnetic forces), as may be surmised from the above analogy with buoyancy forces. If the term is scaled by a constant ε, we find that, given a solution

$$f_0 = F(\xi) \quad , \quad h_0 = H(\xi) \quad \text{for} \quad (1 - \sigma_0)/\rho_0 \quad , \tag{46b}$$

a scaled solution can be derived as

$$f_0 = \varepsilon^{1/4} F(\varepsilon^{1/4}\xi) \quad , \quad h_0 = H(\varepsilon^{1/4}\xi) \quad \text{for} \quad \varepsilon(1 - \sigma_0)/\rho_0 \quad , \tag{46c}$$

while u_0 is scaled by $\varepsilon^{1/2}$. Thus increasing the level of the driving term increases the velocities along the layer and the entrainment; it reduces the thickness of the layer. These results are essentially implicit in the scheme for nondimensionalizing the equations. The characteristic velocity u^0 scales with the square root of the magnetic forces, i.e., like $\varepsilon^{1/2}$, while the thickness scales like $G^{-1/4}$, $\propto u^{0\,-1/2}$, $\propto \varepsilon^{-1/4}$ (see Eqs. (15) for definitions of u^0 and G).

In terms of f_0, $\rho_0\eta_0/P$, the solution of Eq. (44) can be written as

$$h_0 = \int \frac{P}{\rho_0\eta_0} \exp \int - \frac{f_0 P}{\rho_0\eta_0} \, d\xi \, d\xi \quad . \tag{47}$$

By analogy with conventional shear layers, we expect $f_0 < 1$ as $\xi \to -\infty$ and $f_0 > 1$ as $\xi \to +\infty$, i.e., there is entrainment from either side. Then

Eq. (47) implies that h_0 will asymptote to constant values as $\xi \to \pm \infty$, and the two constants of integration may be chosen to satisfy the boundary conditions on h_0. For h_0 = const, we have $(1 - \sigma_0)/\rho_0$ = const. and $\rho_0\eta_0$ = const. With these conditions the asymptotic behavior of Eq. (43) is elementary since it has the form of the Falkner-Skan equations with diverging integral curves as $\xi \to \pm \infty$. Given f_0, $(1 - \sigma_0)/\rho_0, \rho_0\eta_0$ as functions of ξ, Eq. (43) can in principle be solved to yield $df_0/d\xi$ with just two constants of integration. The values of the constants are determined by the need to choose a solution which does not diverge. Although these arguments do not take proper account of the coupling between the equations, they suggest that the boundary conditions (45) are probably necessary and sufficient. (It might be argued that the behavior of Eq. (43) is more like that of the Blasius equation on the hot side, where $\xi \to -\infty$, with $(1 - \sigma_0)/\rho_0 \to 0$ and $df_0/d\xi \to 0$. The equation when linearized about the asymptotic state allows solutions of the form $df_0/d\xi$ = const. Elimination of this type of solution is equivalent to the elimination of the diverging solutions with the Falkner-Skan type of equation.)

3.2 APPROXIMATE METHOD OF SOLUTION

Some elementary, but exact, solutions of Eqs. (43) and (44) can be found when $(1 - \sigma_0)/\rho_0$ has particular functional dependence on h_0. We shall derive a solution for a case where this dependence approximates reasonably to a true property relation.

We start by noting that Eq. (44) can be integrated directly if f_0 is known as a function of h_0. Define therefore

$$f_0 = \partial g/\partial h_0 \quad . \tag{48}$$

However $g(h_0)$ is not a well defined function on the cold side of the layer; $h_0 \to$ const, while f_0 varies since $df_0/d\xi \to$ const $= \sqrt{(1/\rho_0)}$. Our first approximation is to take $\rho_0(-\infty) \to \infty$, which implies that the driving term falls to zero, or the cold gas can have inertia at zero velocity. Implicit also in the analysis is the assumption that both h_0 and f_0 vary monotonically with ξ.

Substituting from Eq. (48) into (44), integrating and setting $g = 0$ where $dh_0/d\xi = 0$, we obtain

$$dh_0/d\xi = - Pg/\rho_0\eta_0 \quad ,$$
$$d/d\xi = - (Pg/\rho_0\eta_0)\, \partial/\partial h_0 \quad . \tag{49}$$

Then Eq. (43) may be written as

$$\frac{Pg}{\rho_0\eta_0} \frac{\partial}{\partial h_0} \{Pg \frac{\partial}{\partial h_0} (\frac{Pg}{\rho_0\eta_0} \frac{\partial^2 g}{\partial h_0^2})\} - \frac{Pg}{\rho_0\eta_0} \frac{\partial g}{\partial h_0} \frac{\partial}{\partial h_0} (\frac{Pg}{\rho_0\eta_0} \frac{\partial^2 g}{\partial h_0^2})$$
$$+ (\frac{Pg}{\rho_0\eta_0} \frac{\partial^2 g}{\partial h_0^2})^2 = \frac{1 - \sigma_0}{\rho_0} \quad . \tag{50}$$

Suppose now that $g(h_0)$ is chosen arbitrarily. Then, knowing $\rho_0\eta_0$ and P as functions of h_0, Eq. (50) gives the dependence of $(1 - \sigma_0)/\rho_0$ for which this assumed form of g is exact. If satisfied that the dependence gives a reasonable approximation to the true property relation, Eqs. (48) and (49) with the assumed $g(h_0)$ may be used to derive $h_0(\xi)$, $f_0(\xi)$, etc.

The choice of a suitable function for g is particularly simple in cases where $(1 - \sigma_0)/\rho_0$ is a symmetric function of $\{h_0 - (1 + h'_\infty)/2\}$, and we take for a first approximation that P and $\rho_0\eta_0$ are constant through the layer. Then inspection of Eq. (50) shows that g should also be a symmetric function of $\{h_0 - (1 + h'_\infty)/2\}$. In what follows assume $h'_\infty = 0$, which may be thought of as being in accord with the approximation $\rho'_\infty = \infty$, although in principle the state where h = 0 can be chosen arbitrarily provided property relations are consistent. $\rho_0\eta_0$ is retained in the analysis so that a suitable average value can be used in the approximate results. We then choose a parabolic function for g:

$$g = ah_0(1 - h_0) \quad , \tag{51}$$

where a is a constant which may be adjusted to give the best fit to the true property relation. Note that g = 0 for $h_0 = 0$ and $h_0 = 1$, the hot and cold sides of the layer. Substitution of Eq. (51) in (50) gives

$$\frac{1 - \sigma_0}{\rho_0} = 2a^4(P/\rho_0\eta_0)^2 \, h_0(1 - h_0) \, \{2(1 + P) \, h_0(1 - h_0)$$

$$+ (1 - P) \, (1 - 2h_0)^2\} \quad .$$

The maximum value, found at h = 1/2, is

$$\left(\frac{1 - \sigma_0}{\rho_0}\right)_{max} = \frac{a^4}{4} \left(\frac{P}{\rho_0\eta_0}\right)^2 (1 + P) \quad ,$$

and we determine a by making the true and approximate forms of $(1 - \sigma_0)/\rho_0$ have the same maximum:

$$g = \left(\frac{1 - \sigma_0}{\rho_0}\right)^{1/4}_{max} \left(\frac{2\rho_0\eta_0}{P}\right)^{1/2}/(1 + P)^{1/4}\, h_0(1 - h_0)$$

for

$$\frac{1 - \sigma_0}{\rho_0} = 8\left(\frac{1 - \sigma_0}{\rho_0}\right)_{max} h_0(1 - h_0)\,\{2h_0(1 - h_0) \tag{52}$$

$$+ (1 - P)\,(1 - 2h_0)^2/(1 + P)\} \quad .$$

Substituting the form of g given in Eqs. (52) we obtain from Eqs. (49) after some algebra

$$h_0 = 1/2 - 1/2 \tanh \beta\xi \quad ,$$

$$-\rho_0 v_0 = f_0 = \left(\frac{1 - \sigma_0}{\rho_0}\right)^{1/4}_{max} \left(\frac{2\rho_0\eta_0}{P}\right)^{1/2} \frac{1}{(1 + P)^{1/4}} \tanh \beta\xi \quad ,$$

$$u_0 = \frac{df_0}{d\xi} = \left(\frac{1 - \sigma_0}{\rho_0}\right)^{1/2}_{max} \frac{1}{(1 + P)^{1/2}} \operatorname{sech}^2 \beta\xi \quad , \tag{53}$$

where

$$\beta = \left(\frac{1 - \sigma_0}{\rho_0}\right)^{1/4}_{max} \left(\frac{P}{2\rho_0\eta_0}\right)^{1/2} \frac{1}{(1 + P)^{1/4}} \quad .$$

The position of $\xi = 0$ has been chosen to be the dividing streamline, $f_0 = 0$.

Taking an elementary property relation for the density, $\rho_0 = 1/h_0$, we can translate to the physical co-ordinate y. Thus

$$h_0 = 1 - 1/2 \exp 2\beta y' \quad ,$$

with (54)

$$2\beta y' \leq \ln 2 \quad .$$

The solution (53) emphasizes the importance of the level of the driving term. Note that the scaling with $(1 - \sigma_0)/\rho_{0\ max}$ agrees with the general result of Eqs. (46b) and (46c). Another interesting feature is the factor $(P/2\ \rho_0\eta_0)^{1/2}$ which appears in β, while β itself is the quantity which controls the length scale. This indicates that the scale is more directly related to the thermal diffusivity than to the viscous. Its further dependence on Prandtl number is weak, entering only through the factor $(1 + P)^{1/4}$.

Eqs. (54) show that the layer ends at finite y' on the cold side. This is due to the approximation that $\rho_0 \to \infty$ and is an extreme illustration of the way in which we expect the scale to shorten as the density increases.

Fig. 8 shows the variation of $(1 - \sigma_0)/\rho_0$ with h_0 for equilibrium air when $h^0 = 8 \times 10^7$ Joule/Kg ($T = 1330^oK$), $h = 3.01 \times 10^5$ Joule/Kg ($T = 300^oK$). The driving term has a humped distribution (i), which reaches a maximum near $h = 4 \times 10^7$ Joule/Kg, the point where the electrical conductivity changes very rapidly with enthalpy. In comparison is drawn an approximating distribution (ii) using the formula of Eqs. (52) with $\{(1 - \sigma_0)/\rho_0\}_{max} = 0.4$ and $P = 0.8$. There is room for improvement but the approximation is not

unreasonable. It is also questionable whether equilibrium values of properties should be used throughout, in which case $(1 - \sigma_0)/\rho_0$ is not known accurately.

Fig. 9 shows the variation of $\rho_0 n_0$ with h_0 under equilibrium conditions; the curve (i) rises steadily to a maximum value of 12 on the cold side. For the approximate solution we take a constant value of 2.5.

In Figs. 10a, b, and c profiles of enthalpy, velocity and f_0 are drawn for the approximate property relations (ii) of Figs. 8 and 9. Note that with the temperatures of (i) we should have $df_0/d\xi \to 0.096$ as $\xi \to +\infty$, lower than the peak value of velocity shown in Fig. 10b but perhaps not insignificant. Fig. 11 shows the enthalpy profile again, but in terms of y'.

Our final analysis of this section aims at giving a more detailed insight into the forces and momentum balances of the shear layer. If the equation of motion (43) is integrated once, we obtain

$$\rho_0 n_0 \frac{d^2 f_0}{d\xi^2} + f_0 \frac{df_0}{d\xi} = \int \{2(\frac{df_0}{d\xi})^2 - (\frac{1 - \sigma_0}{\rho_0})\} d\xi \quad . \tag{55}$$

The sketch of Fig. 12 illustrates the variation of the two terms on the left-hand side of Eq. (55). The velocity peak (zero shear stress) is expected in general to be close to the dividing streamline, where $f_0 = 0$. The terms clearly have a tendency to cancel. Then, making the integral on the right-hand side zero throughout, we would have an indication of velocity magnitudes with

$$u_0 = \frac{df_0}{d\xi} \simeq \sqrt{\left(\frac{1 - \sigma_0}{2\rho_0}\right)} \quad . \tag{56}$$

Eq. (56) underestimates the velocity as $\xi \to \infty$ by a factor $\sqrt{2}$, but differs from the maximum value given by the approximate solution (53) only by a factor $\sqrt{\{(1 + P)/2\}}$. In fact there is a close relation between Eq. (56) and the assumed form (51) for $g(h_0)$, which underlies the approximate solutions. When $P = 1$ and $\rho_0 \eta_0 = \text{const}$, comparison with the energy equation (44) shows that the left-hand side of Eq. (55) is identically zero if f_0 is a linear function of h_0; this corresponds to a parabolic function for $g = \int f_0 \, dh_0$. In general we might expect that the left-hand side of Eq. (55) is small, and Eq. (56) gives a reasonable indication of the variation of velocity with the level of the driving term. (The same technique applied to the natural-convection boundary layer on a flat vertical plate gives good results except in the region where velocity falls off rapidly near the wall.)

The approximate balance of terms suggested above has a simple physical interpretation which is illustrated in Fig. 13. For any control volume of the type shown the change in shear stress is approximately equal to the change in momentum flux carried by the transverse flow, while the difference in magnetic force and pressure is approximately equal to the change of momentum flux carried by the longitudinal flow.

3.3 NUMERICAL SOLUTION

A program was developed by Mr. H. L. Kaye for the numerical computation of solutions to the shear-layer equations (43) and (44). Unfortunately time prevented us from obtaining more than preliminary results, so we shall briefly record here only a few points which may be of interest.

The iterative scheme which was used to solve Eqs. (43) and (44) was based on the following linearization:

$$\frac{d}{d\xi}\left(\rho_0^*\eta_0^*\frac{d^2f_0}{d\xi^2}\right) + f_0^*\frac{d^2f_0}{d\xi^2} = \frac{df_0^*}{d\xi}\left(2\frac{df_0}{d\xi} - \frac{df_0^*}{d\xi}\right) - \frac{1-\sigma_0^*}{\rho_0^*} \quad , \tag{57}$$

$$\frac{d}{d\xi}\left(\frac{\rho_0^*\eta_0^*}{P^*}\frac{dh_0}{d\xi}\right) + f_0^*\frac{dh_0}{d\xi} = 0 \quad , \tag{58}$$

where the superscript * refers to values taken from the previous steps in the iteration. To integrate Eqs. (57) and (58), the differentials were replaced by three-point differences, while the boundary conditions (45) were applied at points where $\pm\,|\xi|$ was considered large enough to make subsequent variation negligible.

The original intention was to solve the equations for model gases which had properties corresponding roughly to air and argon, but which differed principally in having a sharp cut-off in conductivity (for the air model at $h = 4 \times 10^7$ Joule/Kg). A preliminary calculation used property relations denoted by the curves (iii) in Fig. 8 for $(1 - \sigma_0)/\rho_0$ and in Fig. 9 for $\rho_0\eta_0$, while $P = 0.8$ throughout. An interval size of $\xi \simeq 0.6$ was found to be satisfactory with a range approximately $\pm$ 12 (these values are approximate because of a slight scaling adjustment made later to give a better fit to the true $\rho_0\eta_0$). The solution converged to three-figure accuracy after twenty iterations (the analytic solution for the curves (ii) was the first step). Results are shown by the curves marked (iii) in Figs. 10.

Agreement between the numerical and analytic solutions is good. The peak in the curve of $(1 - \sigma_0)/\rho_0$ against h_0 appears to be too sharp to cause a rise in the maximum velocity, but velocity profiles do diverge on the cold side of the layer since the numerical solution now has a nearly correct boundary condition (here taken that $\rho_0 \to 10^2$ as $\xi \to +\infty$, i.e., $u_0 \to 0.1$). The degree of variation put into $\rho_0 \eta_0$ has not made a great difference to the scale.

Some preliminary solutions were computed also for cases corresponding to other values of h^0. Results suggested that the entrainment parameter $f_0(-\infty)$ does not vary greatly, and the enthalpy on the dividing streamline is always slightly less than half the core value.

IV. SHEAR-LAYER DEVELOPMENT

4.1 SEPARATION MECHANISM

As mentioned in Section 1, there is evidence in the experiments of Roman and Myers[4] that vortex streets are formed behind balanced arcs. This and the fact that the drag coefficient is of order unity prompt us to look for mechanisms which might cause the outer part of the shear layer to separate from the inner in a manner analogous to the separation of the boundary layer on a bluff body. An obvious step is to study the development of the shear layers. The stagnation-point solution represented the first terms of power-series expansions in x' (see Eqs. (35)), and in principle the development of the layers could be found from the higher-order terms. However, we find that a complete solution is unnecessary, and indications of the break-down of a boundary-layer approach can be found from a general

analysis of the hot side of the layers. Before giving this analysis in Section 4.2, we present the following physical arguments to clarify our proposal for a mechanism of separation.

The position of a fluid particle in the shear layers follows from the relation:

$$\frac{dy'}{dx'} = \frac{v'}{u'} \quad .$$

In the vicinity of the stagnation point the relation can be written in terms of the stagnation-point variables as

$$\frac{d\xi}{dx'} = - (f_0/x')/(\partial f_0/\partial \xi) \quad .$$

Substituting from the approximate solution (53) we obtain

$$\int \frac{dx'}{x'} = - \int \frac{2d(\beta\xi)}{\sinh 2\beta\xi} \quad . \tag{59}$$

Integrating we obtain

$$x'_e/x' = \tanh \beta\xi \quad ,$$

where x'_e is the value of x' at the point where the fluid particle entered the shear layer. Substitution in Eqs. (53) gives the variation of enthalpy with distance travelled in the shear layer as

$$h_0 = 1/2\ (1 + x'_e/x') \quad . \tag{60}$$

Eq. (60) shows how the rate of change of enthalpy with distance decreases as x'/x'_e increases. Essentially the loss with time, $v'\partial h'/\partial y'$, is bounded, while the particle accelerates continuously so that time spent covering a unit length decreases. A reduction in the rate of enthalpy change with distance appears to be a common feature of thermal boundary layers. Thus, in non-accelerating flow, a decrease in rate of change is found because of the spread of the layer.

The enthalpy of the core is given to a first approximation by

$$h_0 = 1 + h_{1c}x'^2 \quad ,$$

where h_{1c} is the negative quantity of Eq. (46), i.e., the rate of change increases with distance. We therefore suggest that the momentum of the fluid particle may carry it to a region where the enthalpy of the core has become less than that of the particle. The magnetic force will then be greater than the pressure gradient. This excess of adverse magnetic force could cause separation.

There is a possible analogy between the behavior of the shear layers and buoyant plumes. In the same way that the fluid in the buoyant plume is driven upwards by the buoyancy force, the fluid in the shear layers is swept back by the difference between pressure and magnetic forces. With a stable atmosphere (temperature rising with height), the plume reaches a limiting level when the temperatures equalize. The feature of the arc

which corresponds to the temperature variation of the atmosphere is the falling enthalpy of the core. However, in contrast to a two-dimensional plume, the arc layer has one cold side and one hot. The question is whether heat transfer to the cold side is always sufficient to prevent the enthalpy of particles in the layer equalizing with the core.

4.2 FLOW REVERSAL

To develop the speculations of the previous section, we next investigate flow behavior on the core side of the shear layers. Within the framework of the boundary-layer approximation, conditions on the core side approach $u' = 0$, while $\rho_c' v_c'$ and h_c' are functions of x' only. If the equation of motion (25) and the energy equation (26) are linearized on the basis of small perturbations about the core state, they give

$$\rho_c' v_c' \frac{\partial u'}{\partial y'} = \frac{\partial \sigma_c'}{\partial h_c'} (h_c' - h') B_{yc}' + \eta_c' \frac{\partial^2 u'}{\partial y'^2} \quad , \tag{61}$$

$$\rho_c' u' \frac{\partial h_c'}{\partial x'} - \rho_c' v_c' \frac{\partial (h_c' - h')}{\partial y'} = \frac{\eta_c'}{P_c} \frac{\partial^2 (h_c' - h')}{\partial y'^2} \quad . \tag{62}$$

Thus the variation of $(h_c' - h')$ and of u' is governed by ordinary linear differential equations in y', whose coefficients depend on x'. Assume solutions of the form

$$u' = \phi \exp \{(\rho_c' v_c' P_c / \eta_c') \, ky'\} \quad ,$$

$$h_c' - h' = \psi \exp \{(\rho_c' v_c' P_c / \eta_c') \, ky'\} \quad ,$$

where ϕ, ψ and k may be functions of x'. Substitution in Eqs. (61) and (62) and elimination of ϕ and ψ yield

$$k^2(P_c k - 1)(k - 1) = (\rho_c' \eta_c' / P_c^2 \rho_c'^4 v_c'^4)(\partial \sigma_c'/\partial x') B_{yc}' \qquad (63)$$

The hot side of the layer corresponds to $y' \to -\infty$, where $\rho' v' > 0$. Hence Eqs. (61) and (62) will have solutions which asymptote to the core state if $k > 0$. At the stagnation point the right-hand side of Eq. (63) is zero, and its roots are $k = 1/P_c$, $k = 1$, $k = 0$, $k = 0$. The latter two, corresponding to solutions $u' = \text{const} \neq 0$, are rejected.

Moving away from the stagnation point, $\partial \sigma_c'/\partial x'$ becomes non-zero and negative. The typical shape of the curve $k^2(P_c k - 1)(k - 1)$ as a function of k is sketched in Fig. 14, and we see that there is a limited range over which it can have a negative value. If the right-hand side of Eq. (63) is less than the minimum indicated in Fig. 14, the roots k of Eq. (63) must be complex. Such roots represent oscillatory solutions of Eqs. (61) and (62). This implies that the enthalpy in the layer rises above the local core value and the flow reverses direction.

The minimum value of $k^2(P_c k - 1)(k - 1)$ depends only on the core Prandtl number and is plotted in Fig. 15. For $P_c = 1$, the minimum is zero; for values of P_c close to unity, the minimum is approximately $-(P_c - 1)^2/4P_c^2$. If we assume to a first approximation that

$$B_{yc}' = x' \quad , \quad \sigma_c' = 1 + \sigma_{1c} x'^2 \quad ,$$

where σ_{1c} is a negative quantity, the right-hand side of Eq. (63) becomes

$$- 2(\rho_c'\eta_c'/P_c^2\, {}'_c{}^4 v_c'^4)\,(1 - \sigma_c') \quad .$$

Thus the conductivity of the core cannot change greatly before the flow reversals appear, and we therefore approximate ρ_c', etc., at the point of appearance by the stagnation-point values. Then, according to this theory, reversals occur when

$$\sigma_c' = 1 - 1/8\, f_{0c}^4\, (P_c - 1)^2 \quad . \tag{64}$$

It is unfortunate that the result is so sensitive to the Prandtl number, whose value could depend on whether the flow is strictly an equilibrium one or not. This and the fact that the shear-layer equations are linearized about a core state which is approximate leave us with little confidence in the precise prediction of Eq. (64). However, we believe that it does indicate qualitatively that the point at which the enthalpy rises above the core value occurs quite close to the stagnation point, and the effect probably first makes its appearance at the hot edge of the shear layers.

In principle the boundary-layer type of solution should not be continued beyond the point at which flow reversal occurs. The flow no longer has a parabolic character, and the question is whether the basis for a boundary-layer approach to the arc problem has been destroyed by the appearance of reversal close to the stagnation point. We suggest that the qualitative indications of the theory could remain if flow reversal at the edge does not have a strong effect on the layer as a whole. Sketches of isotherms and streamlines corresponding to this view are shown in Figs. 16a and b.

V. INDUCED-EMF AND HALL EFFECTS

The previous discussion has given some basis for a theory of high-current, low-field arcs, where the emf's induced by the flow and the Hall effect are negligible. We have taken the most elementary form for Ohm's law, namely $\vec{j} = \sigma\vec{E}$, but strictly the rest-frame electric field for a fluid particle can differ from $\vec{E}$ by a quantity of order u^0B^0 in the shear layers (although of lower order in the core), while the rest-frame field for an electron differs further by a quantity of order σ^0EB^0/n_e^0e. The latter is a measure of the Hall effect, which can cause electric current to flow in the plane of variation of the arc ; in turn these currents can give rise to motion along the arc column. It is the purpose of the present section to derive conditions under which the neglect of these effects can be justified and to give a qualitative indication of their action. However, if interested only in high-current, low-field arcs, the reader may omit this section, noting only that the ratio of the above quantities to E is measured by M and H of Eqs. (75). If M and H are small we might crudely expect induced emfs and the Hall effect to be negligible to a first approximation.

Suppose that we can regard the arc as strictly two-dimensional, the pressure gradient along the arc being zero. The Hall effect gives rise to $\vec{E}_H$ and $\vec{j}_H$ in the plane of variation and $\vec{v}_H$ perpendicular to it. We retain the symbols $\vec{E}$ and $\vec{j}$ for the primary components along the column, while $\vec{v}$ refers to velocities in the plane of variation. The complete form of Ohm's law is

$$\vec{j} = (\vec{E} + \vec{v} \times \vec{B} - \vec{j}_H \times \vec{B}/n_e\, e) \quad ,$$

$$\vec{j}_H = (\vec{E}_H + \vec{v}_H \times \vec{B} - \vec{j} \times \vec{B}/n_e\, e + \text{grad}\, p_e/n_e\, e) \quad . \tag{65}$$

We shall assume that $u^0 B^0/E$ and j_H/j are at most of order unity, so that, although there may be significant effects in the shear layers, they are not sufficient to invalidate our previous order-of-magnitude estimates of velocities and thickness.

5.1 THE CORE

To start the discussion assume that (i) the self field due to $\vec{j}_H$ is negligible and (ii) the state is still constant on field lines in the core. These assumptions will be found to be consistent with our conclusions. Due to the low velocities in the core, we still have grad $p = \vec{j} \times \vec{B}$, and with (ii) above it follows that $(\vec{j} \times \vec{B} - \text{grad}\, p_e)/n_e\, e$ is irrotational. These terms can be balanced in Ohm's law by an electric field. Thus the Hall effect only has a tendency to drive currents $\vec{j}_H$ with irrotationality of $(\vec{j} \times \vec{B} - \text{grad}\, p_e)/n_e\, e$ in the shear layers. The Hall current in the core is that required for overall continuity with the shear layers and is therefore small, i.e., $j_{Hc} = O(G^{-1/4} j)$. This fact and the low primary velocity in the core allow us to neglect the Hall effect and the induced emf in the primary component of Ohm's law, so that grad $p = \sigma \vec{E} \times \vec{B}$, as before, and assumption (ii) above is justified. Also, since j_H/j is at most order unity in the shear layers only, the self field due to $\vec{j}_H$ is $O(G^{-1/4})$ less than that due to $\vec{j}$, and assumption (i) is justified.

The low Hall current in the core implies that the energy input is still $\overline{\vec{j}} \cdot \overline{\vec{E}} \simeq \sigma E^2$. Then, the general results for the behavior of the

primary flow in the core are unaffected by induced-emf and Hall effects of O(1) in the shear layers.

The equations governing the secondary flow in the core are

$$\vec{E}_H + \vec{v}_H \times \vec{B} - (\vec{j} \times \vec{B} - \text{grad } p_e)/n_e e = 0 \quad , \tag{66}$$

$$\text{curl} \quad (\vec{j}_H/\sigma) = \text{curl} \quad (\vec{v}_H \times \vec{B}) \quad , \tag{67}$$

$$\text{div } \vec{j}_H = 0 \quad , \tag{68}$$

$$\rho \frac{d\vec{v}_H}{dt} = \vec{j}_H \times \vec{B} \quad . \tag{69}$$

In Eq. (66) $\vec{j}_H/\sigma$ is dropped on the grounds that it is $O(G^{-1/4})$. However, E_H must be strictly irrotational, and taking the curl of the full form of Ohm's law yields Eq. (67). Since the core is convection dominated, viscous terms can be dropped from Eq. (69). However, the low magnetic force of the core is equally effective in inducing secondary flow as the greater forces in the layers since the residence time in the core is increased by a factor $O(G^{+1/4})$. The magnetic-force term is therefore retained in Eq. (69). If j_H in the core is $O(G^{-1/4}j)$, v_H may change there by $O(u^0)$.

From the approximate Ohm's law (66) $\vec{E}_H$ is perpendicular to $\vec{B}$, and therefore field lines in the core are lines of constant electric potential.

If $\vec{v}_H \times \vec{B}$ is comparable to $\vec{E}_H$, Eq. (66) shows that it must be irrotational, which requires v_H constant on the field lines. Then the

equation of motion (69) by analogy with the enthalpy equation must have $\vec{j}_H \times \vec{B}$ constant on field lines. The latter condition is incompatible with curl $\vec{j}_H/\sigma = 0$, and therefore $\vec{v}_H \times \vec{B}$ cannot be strictly irrotational. However, only a small departure from v_H = const on field lines gives sufficient rotation to allow $\vec{j}_H \times \vec{B} \simeq$ const. (To strengthen the argument, we note that a rotational part of $\vec{v}_H \times \vec{B}$ which is $O(v_H B)$ induces currents $O(\sigma v_H B)$. The damping time for this rotation, according to Eq. (69), is $O(\rho/\sigma B^2)$. The residence time in the core is much greater if $(\sigma B^2 R/\rho u^0)G^{1/4} >> O(1)$, i.e., with the definition of u^0 in Eq. (2), if $(u^0 B/E)\, G^{1/4} >> 1$. We shall show later that $v_H/E_H = O(u^0/E)$, so that the rotation is rapidly damped when $\vec{v}_H \times \vec{B}$ is comparable to $\vec{E}_H$ provided we use the assumption underlying the boundary-layer approach, $G^{1/4} >> 1$.)

If $v_H \times B$ is of order j_H/σ, the induced emf is negligible in Ohm's law, so that a condition of irrotationality is no longer imposed. Details of the core flow must be found from the simultaneous solution of Eqs. (67), (68) and (69).

5.2 THE SHEAR LAYERS

Now consider the shear layers, where in general the full form of Ohm's law (65) must be used. With the assumption that no induced-emf term or Hall term is significantly greater than $\vec{E}$, there is no change to our previous conclusion that the electromagnetic energy term in the enthalpy equation (14) is negligible. Differences arise in the magnetic-force term of the momentum equation (13), from the fact that there is a momentum equation for $\vec{v}_H$, and the primary motion is coupled to the secondary through the induced-emf terms in Ohm's law.

Across the shear layers the degree of ionization changes rapidly, and the electron-pressure gradient can be large although the total pressure of the gas does not change significantly. If the gas pressure were to be strictly constant everywhere, p_e and n_e could be regarded as functions of temperature only, and $(\text{grad } p_e)/n_e$ e would be irrotational, i.e., the tendency of electrons to diffuse would be counteracted by an electric field only. To find what happens with the appropriate 'incompressible' approximation, where the pressure is nearly constant, we write

$$p_e = \gamma p, \tag{70}$$

where γ is the ratio of number of electrons to total number of particles. Then, relating p_e to its value at the same γ but $p = p^0$, the stagnation pressure, we have

$$p_e(\gamma, p) \simeq p_e(\gamma, p^0) + \left(\frac{\partial p_e}{\partial p}\right)_\gamma (p - p^0) \quad ,$$

$$\simeq p_e(\gamma, p^0) + \gamma(p - p^0) \quad , \tag{71}$$

where it assumed that $(p - p^0) \ll p^0$, and γ in the last term may be evaluated at p^0. Similarly

$$n_e(\gamma, p) \simeq n_e(\gamma, p^0) + \frac{\gamma}{k}\left(\frac{\partial(p/T)}{\partial p}\right)_\gamma (p - p^0) \quad , \tag{72}$$

where we have used the fact that $n_e = \gamma p/kT$. Substituting Eqs. (71) and (72) in the pressure-gradient term and using the fact that $p - p^0$ is small, we obtain

$$\frac{\text{grad } p_e}{n_e e} \simeq \frac{\text{grad } p_e(\gamma, p^0)}{n_e(\gamma, p^0)\, e} + \frac{\text{grad } \gamma(p - p^0)}{n_e(\gamma, p^0)\, e}$$

$$- \frac{(p - p^0)}{n_e^2 e} \frac{\gamma}{k} \left(\frac{\partial(p/T)}{p}\right)_\gamma \text{grad } (\gamma, p^0) \quad ,$$

$$\simeq \left.\frac{\text{grad } p_e}{n_e e}\right|_{p=p^0} + \gamma \frac{\text{grad } (p - p^0)}{n_e e}$$

$$+ \frac{(p - p^0)}{n_e e} \frac{p}{T} \left(\frac{\partial T}{\partial p}\right) \text{grad } \gamma \quad , \qquad (73)$$

where $p - p^0$ may be taken as constant across the layer and evaluated from the pressure gradient in the core, and the remaining thermodynamic quantities can be evaluated at pressure p^0. The first term in Eq. (73) being irrotational gives rise to a large but unimportant electric field. In the last term grad γ is $O(1/\delta)$. But the transverse current density is of small order since the outer edge of the layer is non-conducting, so that the effect of the y-component of the term must be counteracted by E_{Hy}. To maintain irrotationality, the variation of E_{Hx} across the layer would be $O(G^{-1/4} E_{Hy})$, i.e., the variation could be important if the strong gradient

in γ gives rise to large values of E_{Hy}. However γ varies rapidly with temperature and only moderately with pressure in partially ionized gases. It follows that $(\partial \ln T/ \partial \ln p)_\gamma$ is small. We therefore take the last term to be small enough for the variation in E_{Hx} to be negligible across the layer. With this assumption, we also have the longitudinal component of the term negligible. For our purposes then the important term in Eq. (73) is the second, which gives rise to currents along the layer.

In developing a suitable form of Ohm's law in the layers to find the magnetic forces there and the total Hall current crossing the core, we need expressions only for the x- and z-components since the transverse current density is assumed to be negligible. We use also the facts that E and E_{Hx} are constant across the layer for irrotationality (the only term which might invalidate this condition being the last of Eq. (73) discussed above), that u and j_{Hx} in the core are less than the layer values by a factor $O(G^{-1/4})$ by continuity, and that B_y is constant across the layer. Then

$$j = \sigma(j_c/\sigma_c + uB_{yc} - j_{Hx}B_{yc}/n_e\, e) \quad ,$$

$$j_{Hx} = \sigma\{(v_{Hc} - v_H)\, B_{yc} - (\frac{j_c}{n_{ec}} - \frac{j}{n_e})\, B_{yc}/e$$

$$+ (\frac{\gamma_c}{n_{ec}} - \frac{\gamma}{n_e})\, j_c B_{yc}/e\} \quad . \tag{74}$$

In addition to the non-dimensional quantities of Eqs. (15) we introduce

$$v_H' = v_H/u^0 \quad , \quad n_e' = n_e/n_e^0 \quad , \quad H = \sigma^0 B^0/n_e^0 e \quad , \quad M = u^0 B^0/E \quad , \tag{75}$$

but we shall not refer γ to a standard value since it is already non-dimensional and O(1). Then the equations of motion become

$$\rho' u' \frac{\partial u'}{\partial x'} + \rho' v' \frac{\partial u'}{\partial y'} = \{(\sigma_c' - \sigma') B_{yc}' - M \sigma' u' B_{yc}'^2$$

$$+ MH \sigma'^2 B_{yc}'^3 (v_{Hc}' - v_H')/n_e'$$

$$- H^2 \frac{\sigma'^2 \sigma_c' B_{yc}'^3}{n_{ec}'} \left(\frac{1 - \gamma_c}{n_{ec}'} - \frac{1 - \gamma}{n_e'}\right)\}/\left(1 + \frac{H^2 \sigma'^2 B_{yc}'^2}{n_e'^2}\right)$$

$$+ \frac{\partial}{\partial y'} \left(\eta' \frac{\partial u'}{\partial y'}\right) \quad , \tag{76}$$

$$\rho' u' \frac{\partial v_H'}{\partial x'} + \rho' v' \frac{\partial v_H'}{\partial y'} = \{M\sigma'(v_{Hc}' - v_H') B_{yc}'^2 - H \sigma' B_{yc}'^2 \left(\frac{\sigma_c'}{n_{ec}'} - \frac{\sigma'}{n_e'}\right)$$

$$+ H \sigma' \sigma_c' B_{yc}'^2 \left(\frac{\gamma_c}{n_{ec}'} - \frac{\gamma}{n_e'}\right) + MH \sigma'^2 u' B_{yc}'^3/n_e'\}/(1 + H^2 \sigma'^2 B_{yc}'^2/n_e'^2)$$

$$+ \frac{\partial}{\partial y'} \left(\eta' \frac{\partial v_H'}{\partial y'}\right) \quad . \tag{77}$$

The complexity of Eqs. (76) and (77) is daunting, but we can note immediately that the additional terms in Eq. (76) do not affect the

stagnation-point solution. When the series of Eqs. (35) and (36) are substituted, the first contribution of the additional terms gives the power x'^3 in comparison to the x'-dependence of $(\sigma_c' - \sigma')\, B_{yc}'$. Physically, the reason is the smallness of the transverse component of the magnetic field near the stagnation point.

5.3 QUALITATIVE RESULTS

Take the condition $H = 0$, $M \neq 0$, i.e., neglect the Hall effect. We can consider that the term $M\, \sigma' u' B_{yc}'^2$ in Eq. (76) is roughly equivalent to reducing the driving term $(\sigma_c' - \sigma')\, B_{yc}'$ in Eq. (25), where the induced emf is neglected. The theory of the stagnation-point layer suggests that, with lower forcing, velocities are reduced and the layer is thickened (see Eqs. (47) and (48)). Note that the latter expectation is contrary to the behavior of Hartmann channel flows.

Now take the condition $M = 0$, with $H \neq 0$, but small, so that $H^2 \ll 1$, i.e., we consider the Hall effect as a small perturbation and neglect the induced emf. The conditions are sufficient to ensure that the influence of the Hall effect is of second order of smallness in the longitudinal equation of motion (76). We have already seen (Section 5.1) that the Hall effect has no influence on the primary flow in the core. Therefore the primary flow and distribution of enthalpy are unaffected at this level of the Hall effect.

Eq. (77) is now merely a linear equation for v_H' with the form

$$\rho' u' \frac{\partial v_H'}{\partial x'} + \rho' v' \frac{\partial v_H'}{\partial y'} = H\, \sigma' B_{yc}'^2 \left\{ - \frac{\sigma_c'}{n_{ec}'} + \frac{\sigma'}{n_{ec}'} \right.$$

$$\left. + \sigma_c' \left(\frac{\gamma_c}{n_{ec}'} - \frac{\gamma}{n_e'} \right) \right\} + \frac{\partial}{\partial y'} \left(\eta' \frac{\partial v_H'}{\partial y'} \right) \quad . \tag{78}$$

Eq. (78) has an obvious resemblance to that for the primary flow in the shear layers. The driving term is similar in that it is zero at the edges of layers and peaks within it. However, it falls off more rapidly towards the cold side, being zero where $\sigma' = 0$. At low degrees of ionization, the electrical conductivity is directly proportional to the number of electrons, resistance to current flow being provided by electron-atom collisions. At higher degrees of ionization the conductivity becomes limited by electron-ion collisions. It follows that σ'/n_e' decreases with increasing ionization. The quantity γ/n_e' is inversely proportional to the total number density of the particles, and increases with increasing temperature. Hence the driving term is positive unless the temperature (enthalpy) rises above the core value. Note also that the Hall current lies predominantly in the x'-direction.

The core equations (67) - (69) are also linear in v_H'. Because of the linearity, we split v_H' into two parts:

$$v_H' = v_H^* + v_H^{**} \quad , \tag{79}$$

where

$$\begin{aligned} &v_H^* \text{ satisfies Eq. (78) in the layers,} \\ &v_H^* = 0 \text{ in the core,} \end{aligned} \tag{80}$$

and

$$\begin{aligned} &\rho' u' \frac{\partial v_H^{**}}{\partial x'} + \rho' v' \frac{\partial v_H^{**}}{\partial y'} = \frac{\partial}{\partial y'} \left(\eta' \frac{\partial v_H^{**}}{\partial y'} \right) \text{ in the layers,} \\ &\rho \frac{d(v_H^{**} u^0)}{dt} = \vec{z} \cdot (\vec{J}_H \times \vec{B}) \text{ in the core.} \end{aligned} \tag{81}$$

The conditions of Eqs. (80) are roughly analogous to those imposed on the primary flow. We therefore expect v_H^* to be small in the core, but to reach values O(H) directed towards positive z in the layers (assuming the term in braces of Eqs. (80) is O(1)). The major difference from the distribution of primary velocity arises from the fact that v_H^* increases like x'^3 in the vicinity of the stagnation point.

Although $|\vec{j}_H \times \vec{B}|$ is not distributed through the core like $\sigma E^2 - \dot{q}$, Eqs. (81) are roughly analogous to those governing the enthalpy. Hence it is to be expected that the magnitude of v_H^{**} in the core rises from a low value at the rear of the arc to a maximum near the stagnation point. Recalling that the level and direction of $\vec{j}_H$ in the core is determined by overall continuity of current, the magnetic force in the second of Eqs. (81) will accelerate fluid particles in the negative z-direction, and the magnitude will reach O(H). The fact that the Hall current in the layers falls to zero at the stagnation point implies that the core value is zero there, and the distribution of v_H^{**} will be flatter than that of the enthalpy.

The picture which emerges from these crude arguments is one in which the Hall effect causes a secondary flow in the core directed anti-parallel to the primary current (i.e., from cathode to anode). The velocity falls off in the shear layers and may even reverse (the contribution of v_H^*). Sketches of possible current streamlines and contours of v_H = const (arbitrary values) are shown in Figs. 17a and b.

An arc which is slanted with respect to the free stream will differ from those so far discussed in having a component of the external flow

parallel to the z-direction. We could account for this by merely superimposing a uniform velocity throughout the arc. Depending on the slant, the effect may counter or reinforce the tendency of the Hall currents to cause a net flow from cathode to anode. It is interesting to speculate whether the observed slanting of arcs in some experiments has any connection with the Hall effect. Since $u = O\{\sqrt{(\rho_\infty/\rho^0)}\ u^0\}$, Hall velocities are significant in comparison to the free stream when H is only $O\{\sqrt{(\rho^0/\rho_\infty)}\}$. Note, however, that a fluid particle moves a distance in the z-direction $O(HG^{1/4}R)$ when traversing the core; it has to be a long arc for which the assumption of two-dimensionality can be justified.

5.4 THE PARAMETER M

There are some other forms of the induced-emf parameter M of Eqs. (75) which are of some interest. Using the definition of u^0 in Eq. (2), the parameter can be written as

$$M = \sigma^0 B^{0^2} R/\rho^0 u^0 \quad ,$$

$$= (\sigma^0 B^{0^2} R^2/\eta^0)\ (\eta^0/\rho^0 u^0 R) = \sigma^0 B^{0^2} R^2/\eta^0 G^{1/2} \quad . \tag{82}$$

This shows that M is equivalent to an interaction parameter for the internal circulation or to the square of the Hartmann number based on shear-layer thickness.

With the drag condition of Eq. (3), Eq. (82) becomes

$$M = O\{\sqrt{(\rho_\infty/\rho^0)}\ \sigma^0 B^{0^2} R/\rho_\infty u_\infty\} \quad ,$$

$$= O\{(\mu_0 \sigma^0 u_\infty R) \times \sqrt{(\rho_\infty/\rho^0)} \times (B^{0^2}/\mu_0 \rho_\infty u_\infty^2)\} \quad . \tag{83}$$

The last part of the expression is the inverse of the square of the Alfvén number, a parameter which controls the level of the self field (see Eq. (33)). The first part of the expression is a magnetic Reynolds number, which we can expect to be low. Hence it is unlikely that the complications of self-field and induced-emf effects will occur simultaneously.

VI. OVERALL PARAMETERS

6.1 SIMILARITY

For a given gas at a particular state in the free stream, there are two independent variables for the arc as a whole, e.g., the total current

I and the imposed field B_0 (which we suppose uniform). The velocity of the free stream at which a balance is achieved is then a dependent variable.

Consider a family of arcs, all having the same shape, pressure and maximum enthalpy. Suppose also that the enthalpy distribution in the core is similar. We can show that this family will allow any combination of the independent variables I and B_0 if the self field, radiation, induced emfs and Hall effect can be neglected.

Firstly, since the magnetic force in the core $\sigma\vec{E} \times \vec{B}$ depends on temperature only, the pressure distribution will be similar, a necessary condition for compatability with an outer inviscid flow over the particular shape. Secondly, the non-dimensional characteristics of the shear layers depend only on the thermodynamic state of the core (see the boundary conditions of Eq. (28)). The layers have similar characteristics along their length - in particular the position of effective 'separation' is similar, and the enthalpy of the separated outer part is the same for all members of the family. The latter feature is compatible with a condition that the separated flow be nonconducting. (In this discussion it is tacitly assumed that the effective separation occurs nearer the rear of the arc than the point at which the shear-layer enthalpy can rise above the local core value. Thus the core and layer description applies to the major part of the arc, and the layers are given to a first approximation by, say, a local-similarity solution to Eqs. (24) - (29).) Then, to maintain this family, we need only ensure that the entrainment to the layers and the energy input to the core are such that the enthalpy change

across the core is the same for all the arcs. This requires only that the parameter α of Eqs. (15), which according to Eq. (23) controls the enthalpy variation, should be the same for all. Since α depends on R, the one degree of freedom left in the family, namely size of arc, allows its constancy for any values of I and B_0.

If the solution to the arc problem is unique, it must be a member of the above family, provided that the effects of self field, etc., are negligible. We emphasize that the family has the important properties of similar shape and similar distribution of the thermodynamic state for a particular pressure. Pressure variation will cause differences in the property relations applied to the shear layers and core, but the value of the enthalpy in the free stream has much less significance since the characteristics of the shear layers only depend weakly on the density ratio across them.

Because of the similarity in the thermodynamic state of the core, the arc resistance is proportional to the cross-sectional area (the fraction of current passing through the layers if $O(G^{-1/4})$). Thus

$$I/ER^2 = \text{const} \quad . \tag{84}$$

The drag condition gives

$$u_\infty^2 R/IB_0 = \text{const} \quad , \tag{85}$$

if we neglect dependence of the drag coefficient on Reynolds number, an

assumption consistent with neglecting details of the flow beyond the effective separation. The scaling law, α = const, gives when we apply Eq. (84) to the definition in Eqs. (15)

$$I^{7/4}/B_0^{1/4}\, R^{9/4} = \text{const} \quad , \tag{86}$$

while G is proportional to IB_0R. Treating I and B_0 as the independent variables we obtain the following laws for the arcs:

$$R \propto I^{7/9} B_0^{-1/9} \quad , \quad u_\infty \propto I^{1/9} B_0^{5/9}\, \rho_\infty^{-1/2} \quad ,$$

$$E \propto I^{-5/9} B_0^{2/9} \quad , \quad G^{1/4} \propto I^{4/9} B_0^{2/9} \quad . \tag{87}$$

From Eqs. (87) we see that the value of the current is the principle control of size and the value of the field that of the balance velocity. The validity of the boundary-layer assumption ($G^{1/4} >> 1$) depends more strongly on the current than the field.

If the proportionalities (87) were universally valid, balanced-arc data for a given gas and pressure could be reduced to a set of constants. The neglected effects, e.g., self field, will cause a departure from these laws. However, when only one effect has to be included, we can obtain a condition for the arcs to be similar, e.g., that the ratio of self field to imposed should remain the same. Thus we must have $\mu_0 I/B_0 R$ = const. for similarity with self field only, E = const with

radiation (proportionality of energy input and radiation at a given state), M of Eqs. (75) = const with induced-emf effects and H of Eqs. (75) = const with Hall effect. Given any one condition, we can apply Eqs. (87), and the similarity laws become

$$
\begin{aligned}
I/B_0^4 &= \text{const. if self field only} \quad , \\
B_0^2/I^5 &= \text{const. if radiation only} \quad , \\
IB_0^2 &= \text{const. if induced emf only} \quad , \\
B_0 &= \text{const. if Hall effect only} \quad .
\end{aligned}
\tag{88}
$$

Under the influence of any one effect, the similarity may be substituted back in Eqs. (88) to eliminate partially the dependence on B_0. Thus, for example, with self field only we obtain

$$R = I^{3/4} \times \text{function } (I/B_0^4) \quad ,$$

$$u_\infty = I^{1/6} \times \text{function } (I/B_0^4) \quad .$$

6.2 CHARACTERISTIC MAP

The theory of arcs given in this report has not reached a sufficiently advanced stage for close quantitative prediction of behavior. However, we shall attempt to give some indication of the values of parameters by essentially order-of-magnitude estimates.

Our first assumption is that the arc is approximately circular with radius equal to that of the nose. The experimental evidence of Roman and Myers[4] suggests this to be untrue; their arcs appeared to become elliptical with major axis (transverse to the free stream) reaching as much as 1.8 times that of the minor. However, even at the highest values of the imposed field, the Alfvén number N, which estimates the importance of the self field (see Eq. (33)), was not less than 2. In the discussion of Section 2.5, we suggested that closed field lines in the core would be inconsistent with a boundary-layer theory. Now, for a given current and cross-sectional area, an elliptic shape with major axis parallel to the applied field lessens the tendency to form closed field lines. It is therefore possible that the observed increase in the ratio of major to minor axes with velocity represents an attempt of the arc to avoid closed field lines as conditions become more nearly suitable for a boundary-layer approximation. For this reason, there does not seem to be sufficient experimental evidence for choosing a shape of arc other than the simplest, i.e., circular, when Alfvén numbers are low.

For our second assumption, we suppose that the enthalpy h^0 at the stagnation point to be determined by a requirement that the separated part of the shear layers should be non-conducting. The enthalpy on the dividing streamline should then have a value at separation such that the conductivity is effectively cut off. Fluid particles will cool between the stagnation point and separation, but, for want of a quantitative theory of the amount of cooling, we apply the condition at the stagnation

point. Then the analytic solutions of Section 3.2 suggest $h^0 = 2h^*$, where h^* is the cut-off enthalpy. We also take h^* to be the enthalpy at the rear of the arc.

Thirdly, we shall, in a similar spirit, merely take the flow across the core to be constant = $\rho^0 v^0$. (A possible improvement would be to use the value of the entrainment parameter given by the solution of Section 3.2 and take the mass flow to be $f_0 \rho^0 v^0$.) Then taking an average for the electromagnetic power less radiation we write

$$\rho^0 v^0 \frac{h^0/2}{2R} = \frac{\sigma^0 E^2 - \dot{q}^0}{2} \quad .$$

Again there is room for improvement on the grounds that the strong dependence of $\dot{q}$ and σ on h could make the use of an arithmetic mean on the right-hand side a poor approximation. The form of the energy equation, however, retains an important feature, namely that E^2 must be greater than $\dot{q}^0/\sigma^0$. Substituting from Eqs. (15) and evaluating properties at $h^0 = 8 \times 10^7$ Joule/Kg for air at one atmosphere ($\dot{q}^0 \simeq 10^9$ watts/m^3 from the data of Kivel and Bailey[6]), we obtain

$$197\, E^{1/4} B^{1/4} / R^{5/4} = E^2 - 1.76 \times 10^5 \quad . \tag{89}$$

For the total current we take $I = \pi R^2 \delta^0 E$, and for the drag condition $\rho_\infty u_\infty^2 R = IB$.

From the above equations a map of arc properties in atmospheric air has been prepared and is given in Fig. 18. With axes I and B_0, we show

full lines of constant radius, constant u_∞ (the associated Mach number is indicated) and constant $G^{1/4}$. Also shown are dashed lines for values of the self-field parameter N^2, the induced emf parameter M, the electric field E (the non-dimensional quantity measuring the ratio of radiation to energy input $\dot{q}_0$ is given in parentheses). The Hall parameter H depends only on the magnetic field, and values are indicated at the side.

In the approximate solution of Section 3.2, the enthalpy in the stagnation-point layer reaches 90% of its core value at $y' = -3.5$ (see Fig. 10a). From Eqs. (15) we have $y = y' RG^{-1/4}$. Therefore it is only in the upper right-hand region of the map that the boundary-layer approach might begin to give reasonable results. Induced emf effects are noticeable there, and the Hall effect could cause significant longitudinal flow, although it is small enough to have little influence on the primary flow (see Section 5.3).

If we take the map at face value in spite of the low values of $G^{1/4}$, it suggests that the self field could have a significant influence up to values of B_0 in the region of 0.1 Wb/m^2. There is a small region near $B_0 = 0.1$ Wb/m^2, I = 200 A, where the simplest kind of arc can be expected, i.e., one for which self field, radiation, induced emfs and Hall effect can be neglected.

It is noteworthy that the principle effect of radiation on the overall properties is to reduce the variation of the electric field in the lower right-hand region of the map.

In the experiments of Roman and Myers[4], imposed fields up to 5×10^{-3} Wb/m^2 and currents in the range 190 to 400 A were used. Their results,

therefore, cover only a small part of the map, and a part where the boundary-layer approximation is poor, and self fields are dominant. However, as the free stream velocity increased from 10 to 18 m/sec, the required field at a current of 300 A increased from approximately 1.7×10^{-3} to 4.9×10^{-3} Wb/m^2. The map gives 2.0×10^{-3} and 6.4×10^{-3} Wb/m^2. At 400 A and 18 m/sec, the map would predict an arc of slightly greater diameter than 1.2 cm, while the experimental data suggested an elliptical shape with major axis 1.12 cm and minor 0.74 cm. The high values of B_0 could be consistent with the apparent over-estimate of the size, and also consistent with an experimental value of E just under 1000 V/m in comparison to the map prediction of just under 600 V/m. Because of the lower value of E, the map gives higher importance to radiation than was indicated by the experiments.

The following qualitative aspects of the experiments are mirrored by the map: The balance velocity for given current increases with field to not quite the half power, and the current decreases slightly with increasing field for given velocity. The arc size depends principally on current, increasing with current for given velocity. At high velocities, the measurements of electric field give velocity increasing with both electric field and current.

VII. CONCLUSIONS AND RECOMMENDATIONS

7.1 CONCLUSIONS

The principle conclusions to be drawn from this theory are as follows:

(i) There will be an internal circulation within the arc with high

velocity, of order $\sqrt{(\rho_\infty/\rho^0)}$ times that of the external stream, at least near the edges of the arc.

(ii) A boundary-layer approach is not strictly valid due to the low values of $G^{1/4}$ encountered in practice. Values of $G^{1/4}$ are nearly sufficient at high, yet practical, fields and currents.

(iii) A solution of the shear-layer equations can be found for the stagnation point. The main feature is a peaked velocity profile. The solution does not depend strongly on the external flow.

(iv) Following the shear layers round the edge of the arc, a condition is approached such that the net force due to pressure gradients and magnetic forces is adverse. This may lead to separation. The start of the phenomenon is seen close to the stagnation point and at the hot edge of a layer.

(v) Self fields and radiation are important influences on behavior in the core of the arc for a wide range of currents and imposed magnetic fields.

(vi) Closed field lines within the arc are inconsistent with the boundary-layer approximation. It is suggested that a strong self field could be an important influence on the shape of the arc.

(vii) At high fields, the influence of induced emfs could reduce circulation and thicken the shear layers.

(viii) At high fields, the Hall effect induces flow along the arc. It is suggested that a net flow occurs from cathode to anode unless the arc is slanted with cathode downstream.

(ix) The overall energy balance depends on the electromagnetic input and radiation in the core, and on the entrainment to the shear layers. The latter and therefore the energy balance are only weakly dependent on the external conditions.

(x) The theory suggests universal scaling laws for arcs in the absence of self field, radiation, induced emfs and Hall effect. Conditions for similarity can be derived when only one of these effects is present.

Finally we may ask in what respect is this theory significantly different from those where motion in the arc is neglected. Since high values of $G^{1/4}$ are not obtained in practice, a scale length equal to arc size rather than shear-layer thickness cannot give a very different answer for the heat conducted to the outer flow. As in theories which neglect motion, we associate the enthalpy at the boundary with that giving effective cut-off in electrical conductivity. However, previously, heat transfer from the boundary to the outer flow has been assessed from standard fluid-mechanic data for cylinders. These data are well verified for small temperature differences, but it is questionable whether they can be used under arc conditions. If the density is much less at the wall of a solid cylinder than it is in the outer flow, we might expect velocity overshoots in accelerated boundary layers (by the arguments of Section 2.1 velocities might reach u^0 in our terminology). Then the character of the boundary layer will be rather similar to the outer part of the shear layers in the present analysis. It is therefore possible that with correct heat-transfer data the two approaches would not lead to a great difference in the quantitative prediction of overall parameters.

7.2 EXPERIMENTAL RECOMMENDATIONS

While it is appreciated that the detailed behavior inside an arc is not easily investigated, there are some overall or external measurements which could lead to a better understanding of balanced arcs. A few points are worthy of special mention:

(i) In any experiment designed to check the theory, the two-dimensionality of the arc must be established by varying the electrode spacing. Note that longitudinal flows induced by the Hall effect at high fields may make the condition more difficult to achieve.

(ii) Conditions must be chosen so that buoyancy forces are not significant (although the theory could be extended to allow for these forces in the case of a horizontal arc in a vertical flow).

(iii) Although the experiments of Roman and Myers[4] have given some evidence to show that the external stream does not enter the arc, further direct confirmation is desirable - possibly using the same technique with observation of injected particles. Even if the assumption that the arc is a region of closed streamlines proves correct, it is important to verify a feature implicit in most attempts at an arc analysis, namely that the boundary between external and internal flow coincides with cut-off in electrical conductivity. It is not beyond the bounds of possibility that a closed, double-vortex pattern in the region of the arc could have streamlines which reach outside the area of luminosity. A test for this would be to inject particles <u>downstream</u> of the arc and to see whether they are drawn into it.

(iv) There is a need to make further comparison of the present overall predictions with existing experimental results, i.e., with those of moving arcs. However, it does seem that there is a paucity of data on long arcs whose condition has been carefully observed - especially ones which are stationary with respect to the electrodes. There is a need for complete maps, of the type we have tried to derive from the theory, to be made from experimental data, particularly in regard to dimensions and actual electric field, as measured by probes within the arc.

If the present hypotheses are not refuted, the following recommendations might lead to a further advance in theory or more detailed interpretation of the results by allowing a more precise integration of the core energy equation.

(v) As much information as possible on the shape of the arc is desirable - especially how the shape is affected as the parameters N^2 and G are varied. The self field outside the arc could be measured, and a direct indication of field reversal and its influence on arc shape obtained.

(vi) It is a difficult experimental task to find the position of separation, but an attempt should be made if flow-visualization techniques can be perfected sufficiently.

7.3 RECOMMENDATIONS FOR FURTHER THEORETICAL WORK

(i) There is a need for a stability analysis of the core (see Section 2.2).

(ii) Further questions on stability can be raised. Firstly, what is the condition for stability of the shear layers (although, having low effective Reynolds number, there may be sufficient dissipation to damp disturbances under practical conditions)? Secondly, as $G^{1/4} \to 0$, the shear

layers represent a boundary where light fluid is pressed against heavy by magnetic forces. It is possible that a Rayleigh-Taylor type of instability could exist.

(iii) Further work on the continuation of the shear layers (possibly using an assumption of local similarity) might lead to a more precise definition of separation and show whether present ideas on shear-layer behavior are tenable. The separation point must be established if theories of arc shape are to be developed. There is perhaps little hope for a complete description of streamline closure at the rear of the arc.

(iv) Given a better knowledge of arc shape, there will be scope for further work on magnetic field patterns to determine whether closed field lines occur.

REFERENCES

1. W. T. Lord, "Some magneto-fluid-dynamic problems involving electric arcs", RAE TN Aero. 2909, 1963.

2. T. W. Myers and W. C. Roman, "Survey of investigations of electric arc interactions with magnetic and aerodynamic fields", ARL 66-0184, September 1966.

3. A. M. Kuethe, R. L. Harvey and L. M. Nicolai, "Model of an electric arc balanced magnetically in a gas flow", AIAA 5th Aerospace Sciences Meeting, paper no. 67-96, January 1967.

4. W. C. Roman and T. W. Myers, "Investigation of electric arc interaction with aerodynamic and magnetic fields", ARL 66-0191, October 1966. (See also AIAA 5th Aerospace Sciences Meeting, paper no. 67-98, January 1967.)

5. R. J. Arave, T. C. Peng, E. A. Brown and W. M. Howard, Boeing report no. D2-11781.

6. B. Kivel and K. Bailey, "Tables of radiation from high-temperature air", AVCO report no. 21, 1957.

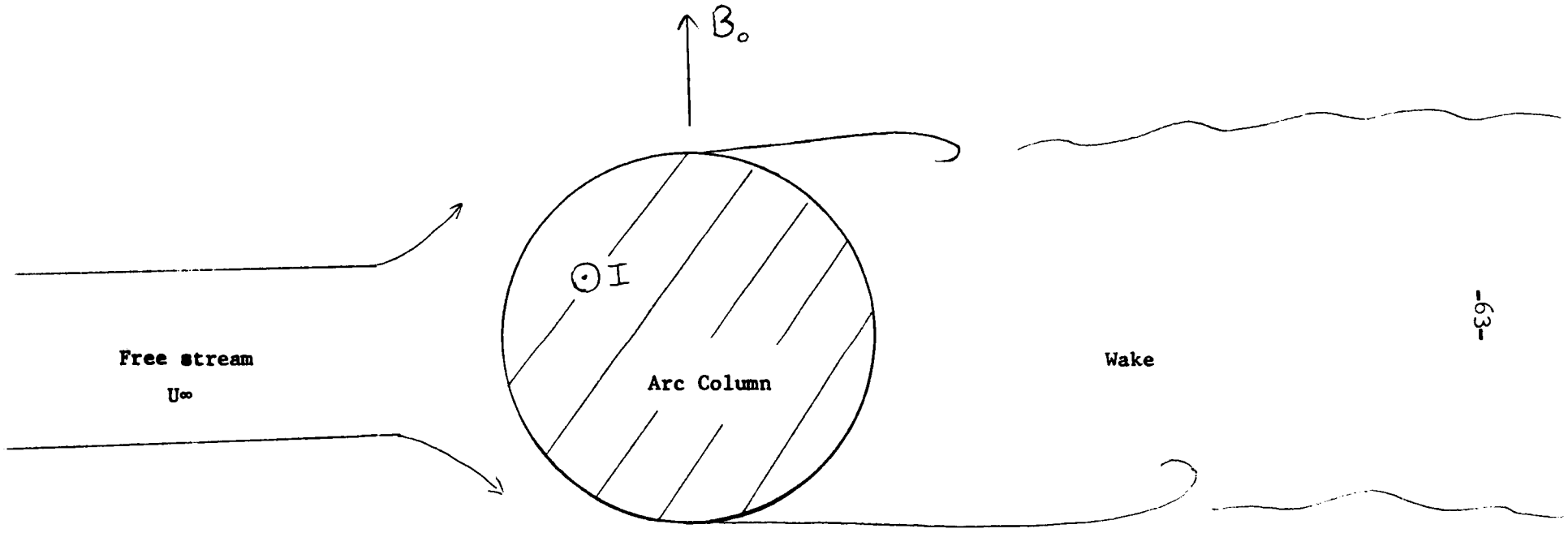

Fig. 1. The balanced arc

Magnetic flux

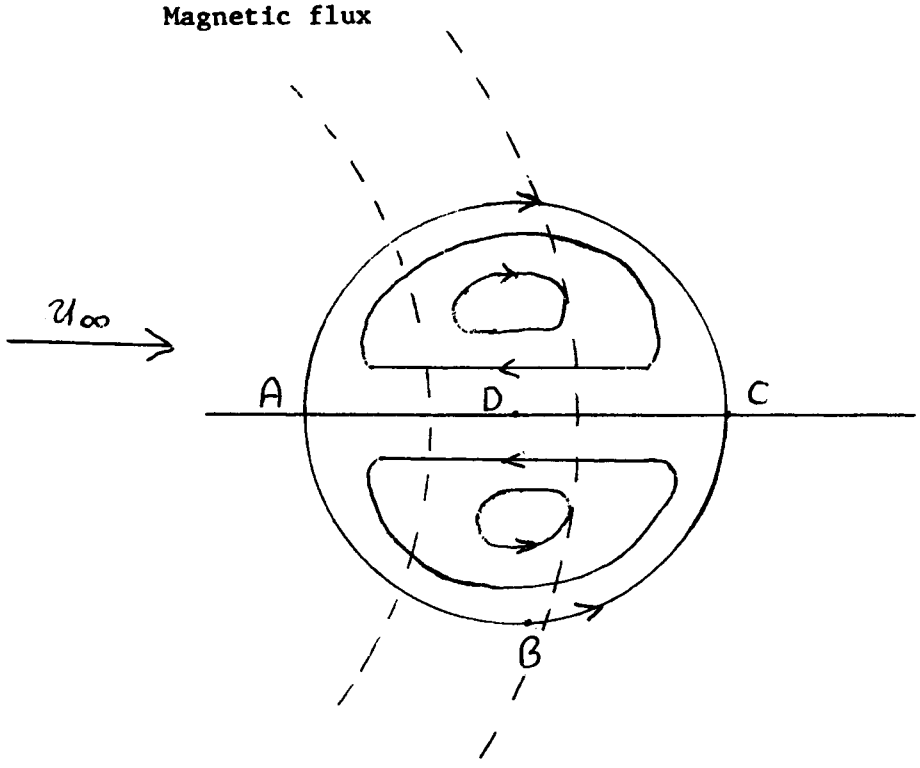

Fig. 2a. Vortex pattern in the arc column

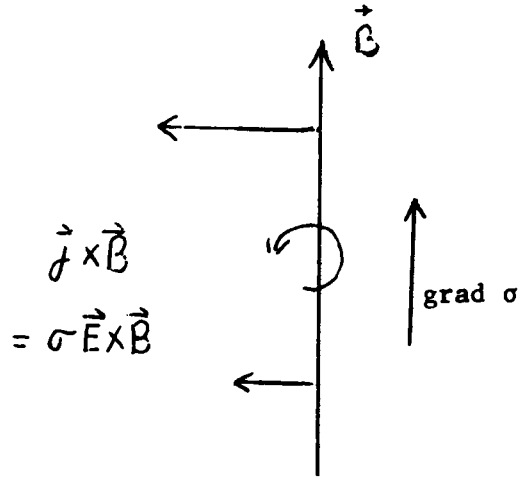

Fig. 2b. Rotational effect of the magnetic forces

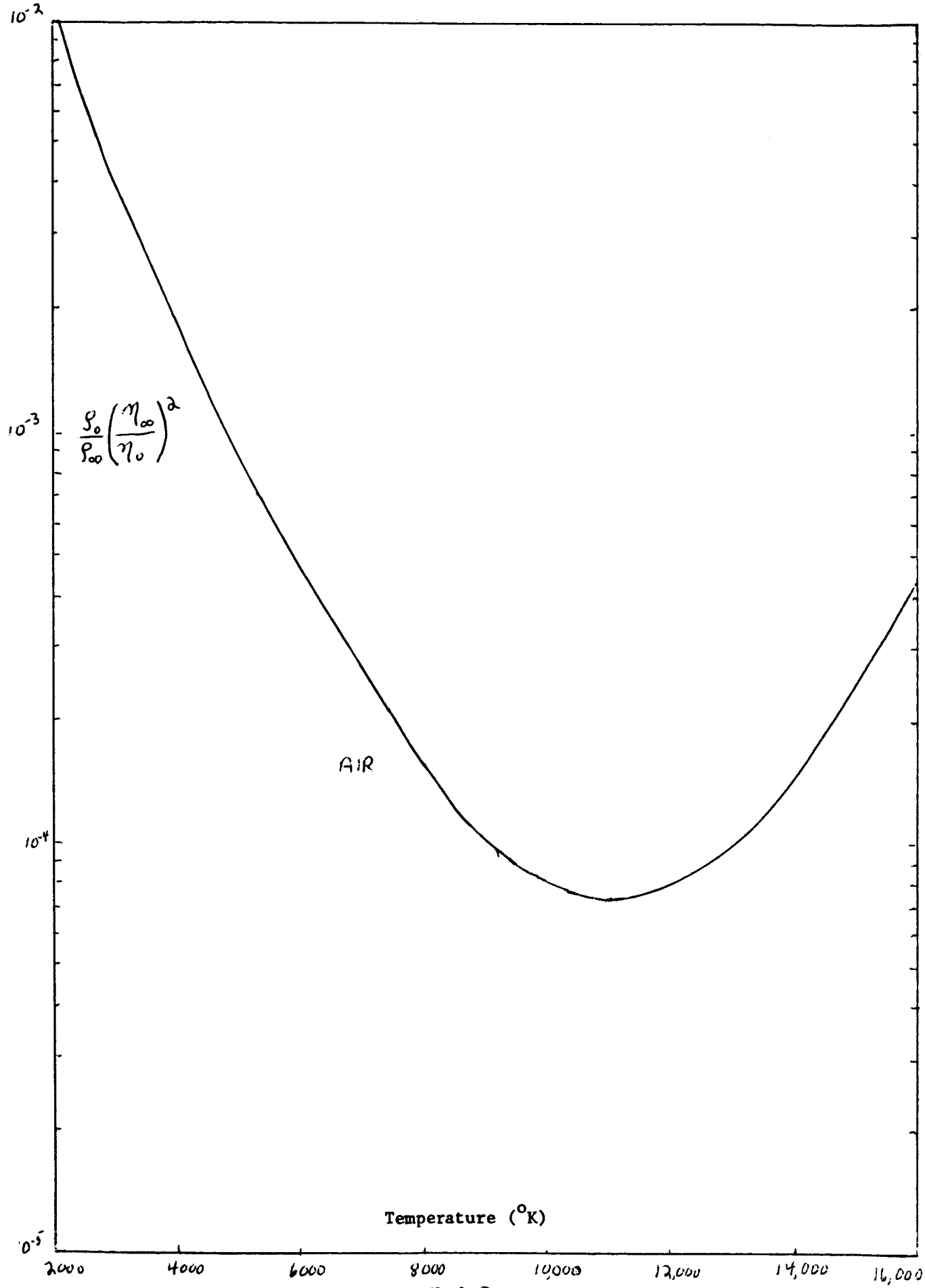
10^{-2}
10^{-3}
10^{-4}
10^{-5}
$\frac{\rho_0}{\rho_\infty}\left(\frac{\eta_\infty}{\eta_0}\right)^2$
AIR
Temperature (°K)
2000
4000
6000
8000
10,000
12,000
14,000
16,000

FIG 3

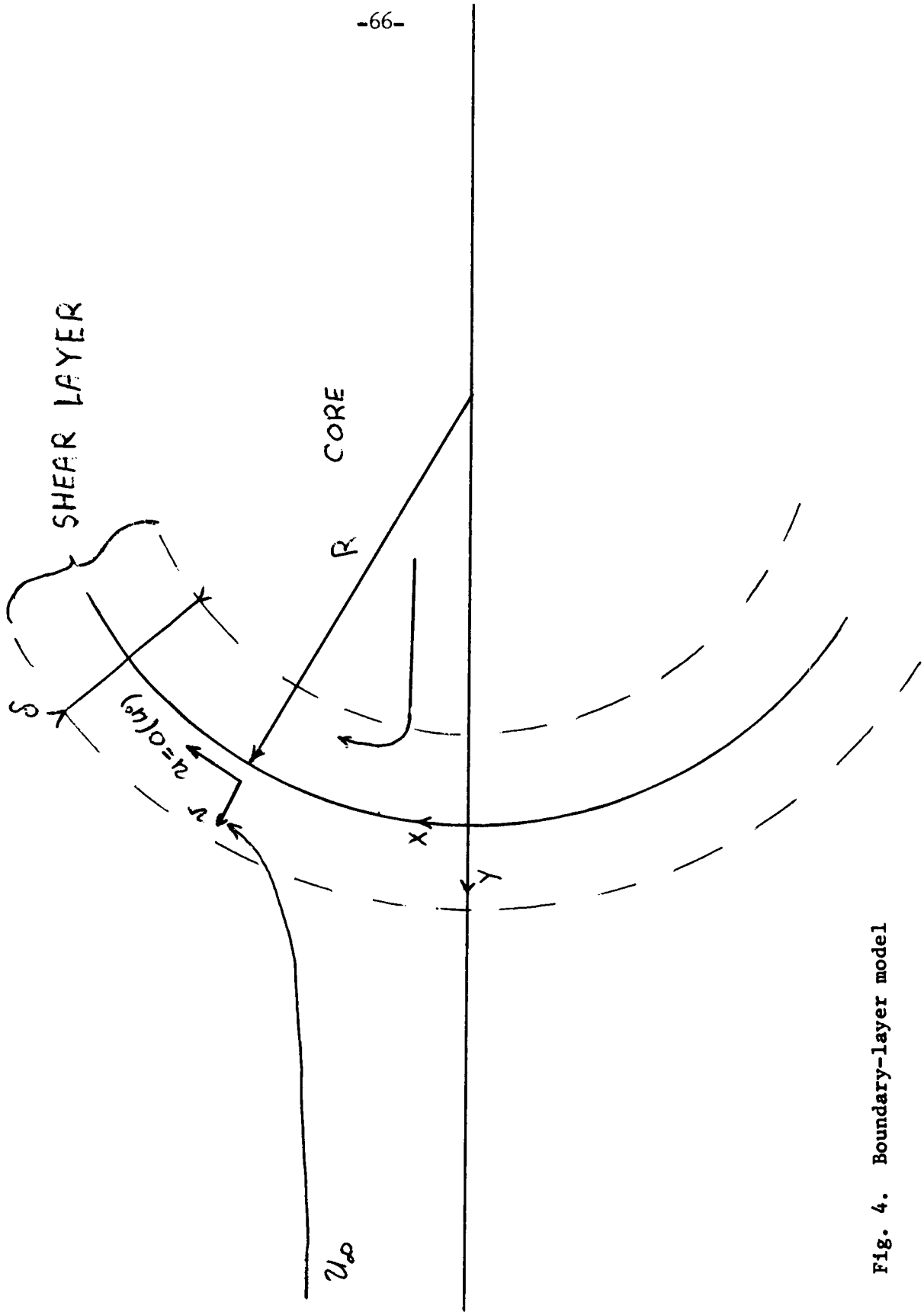

Fig. 4. Boundary-layer model

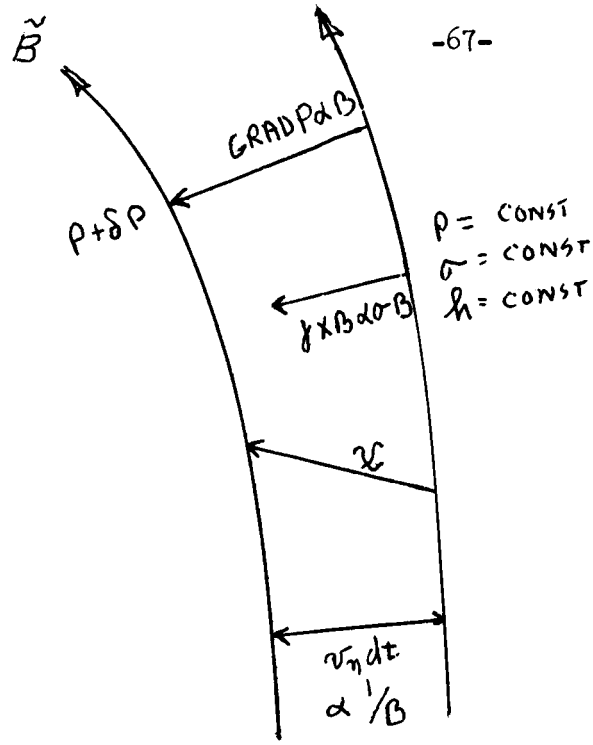

Fig. 5a. Core behavior

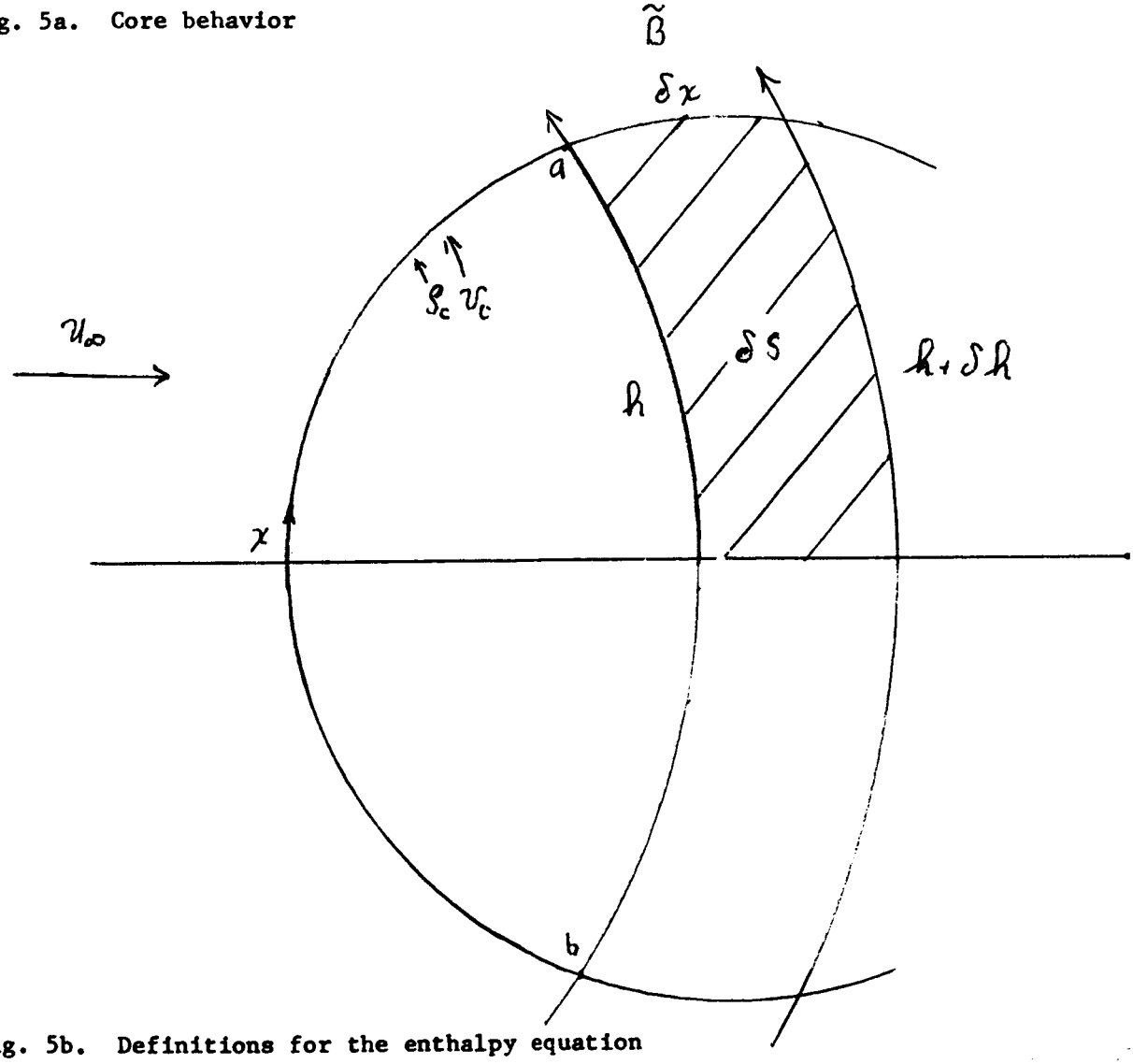

Fig. 5b. Definitions for the enthalpy equation

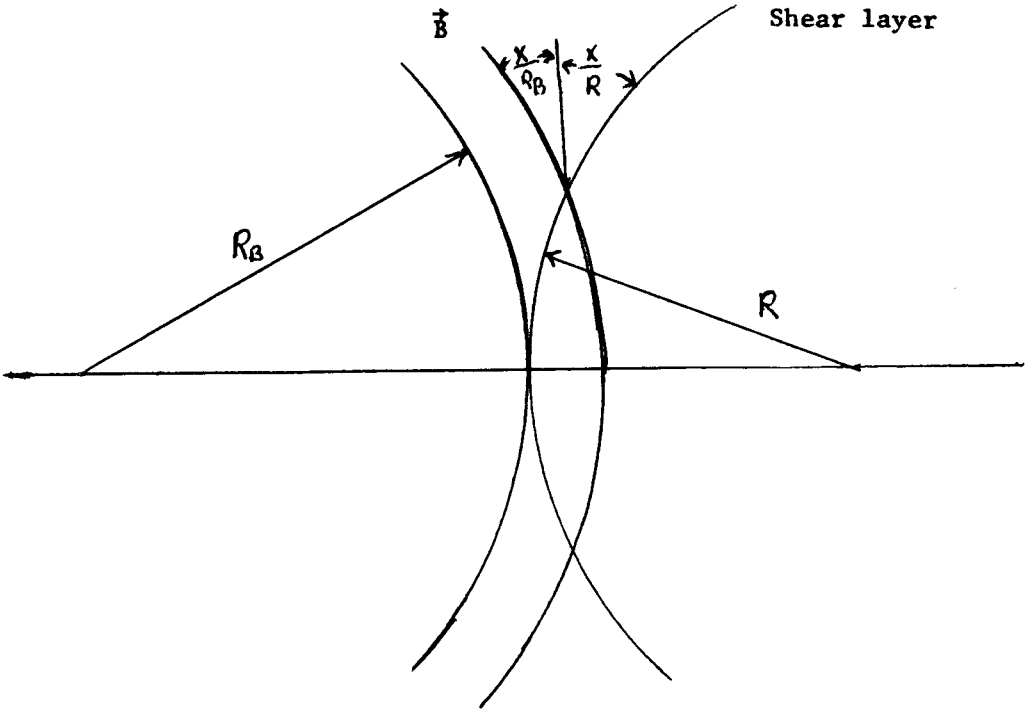

Fig. 6a. Field lines near the stagnation point

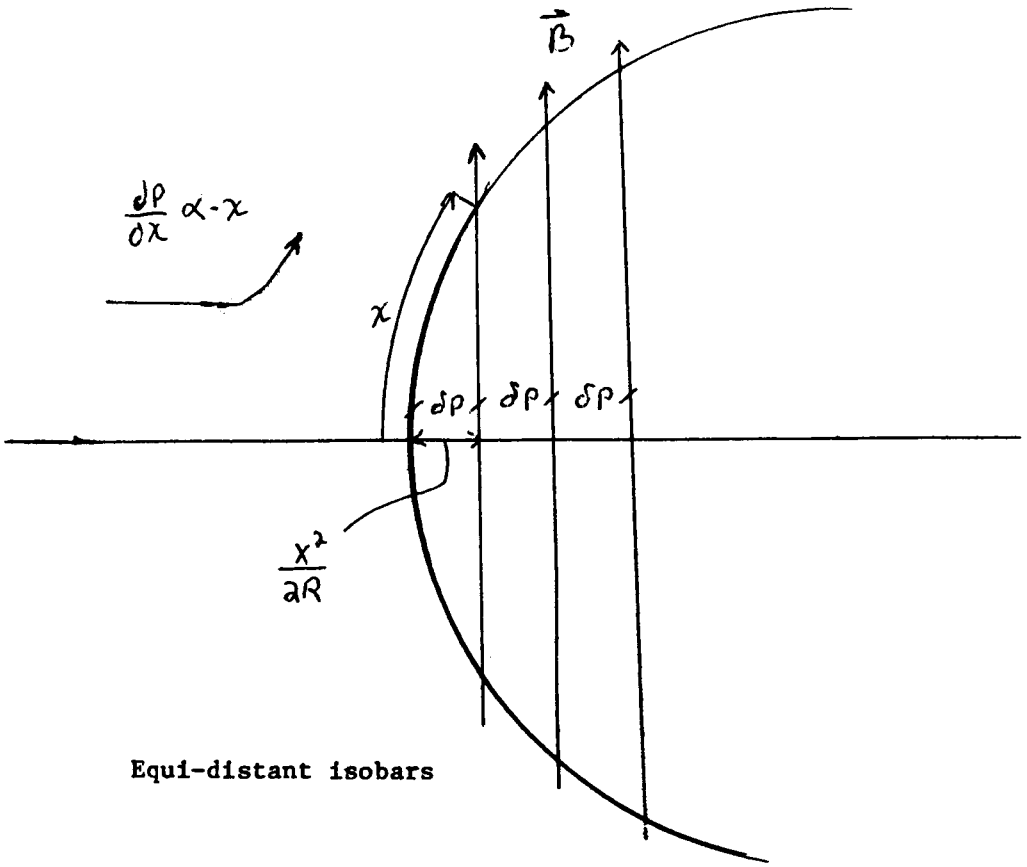

Fig. 6b. Equi-distant isobars

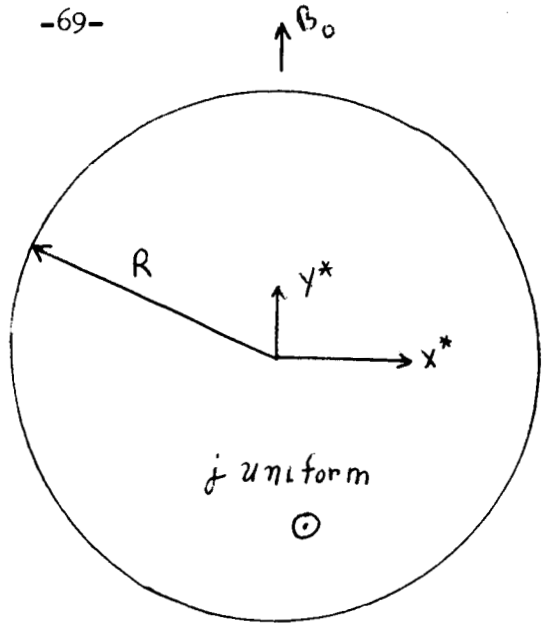

Fig. 7a. Co-ordinates for the self field

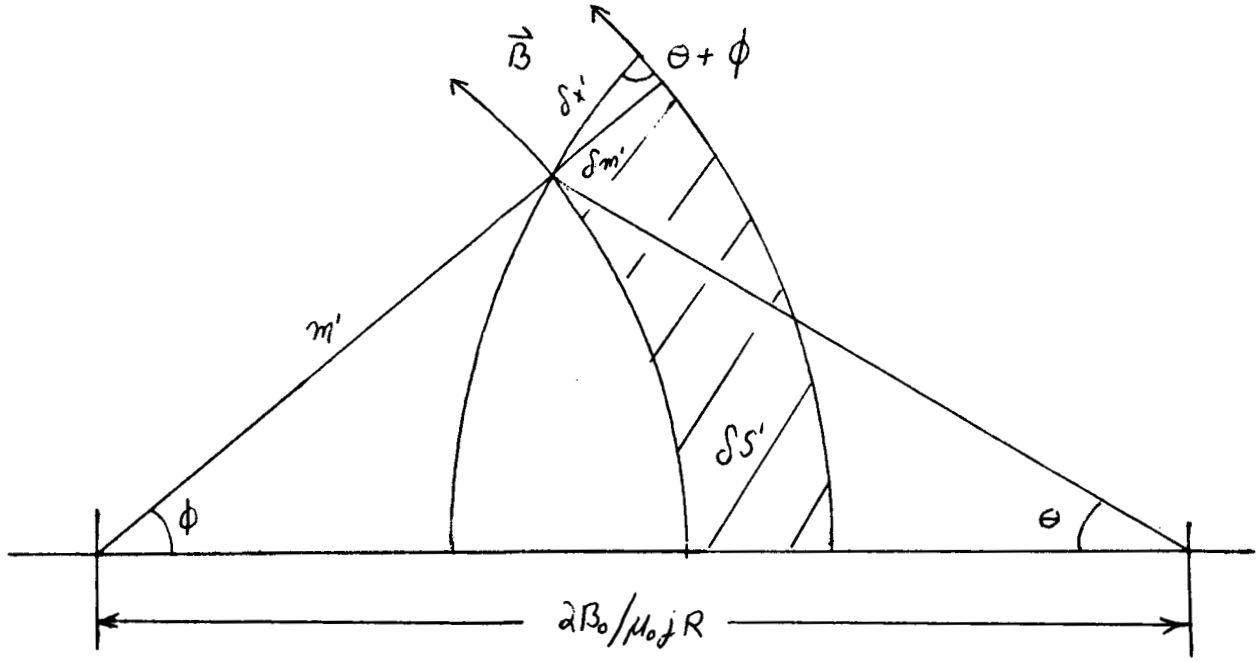

Fig. 7b. Trigonometry of the field lines

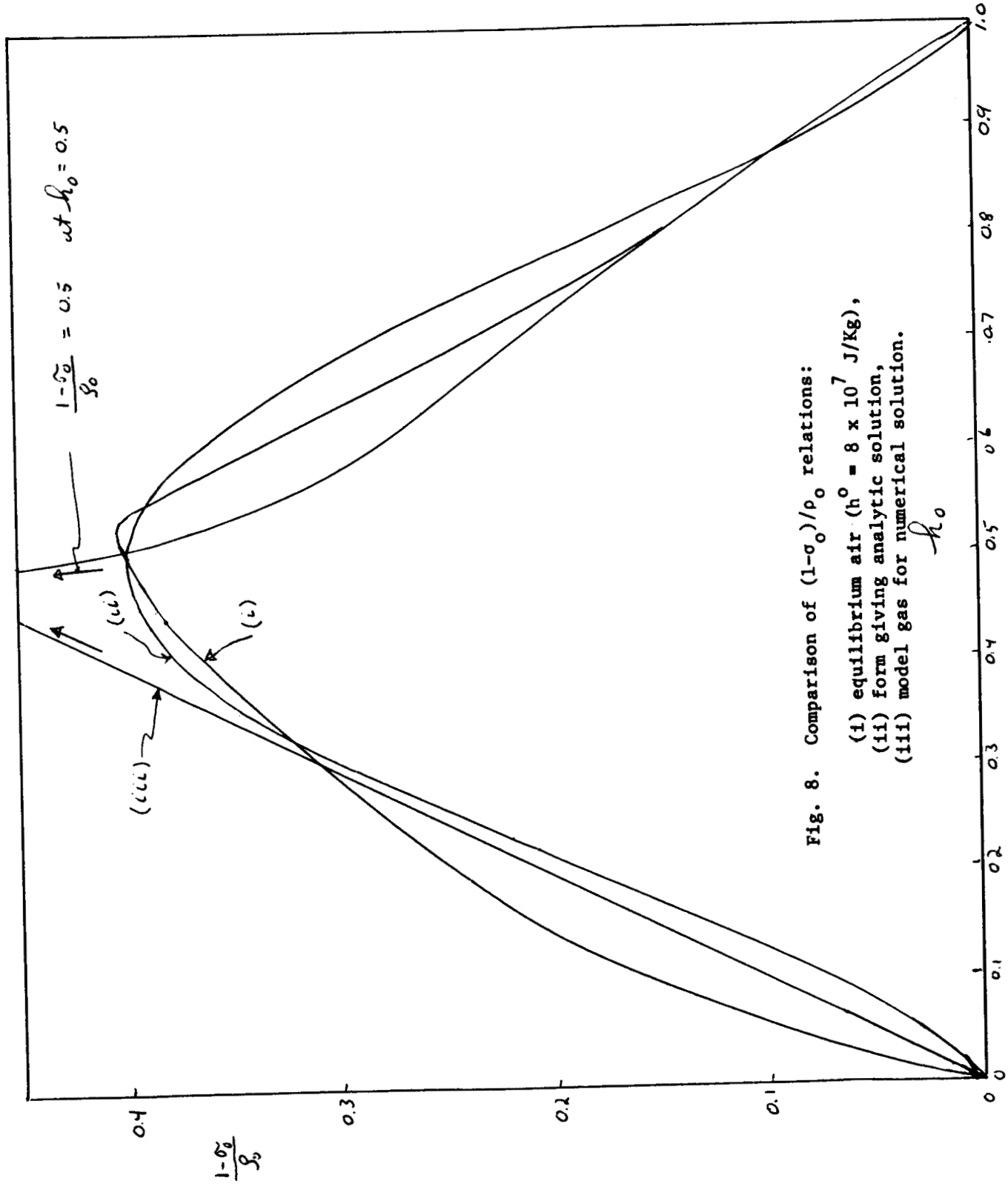

Fig. 8. Comparison of $(1-\sigma_0)/\rho_0$ relations:
(i) equilibrium air ($h^0 = 8 \times 10^7$ J/Kg),
(ii) form giving analytic solution,
(iii) model gas for numerical solution.

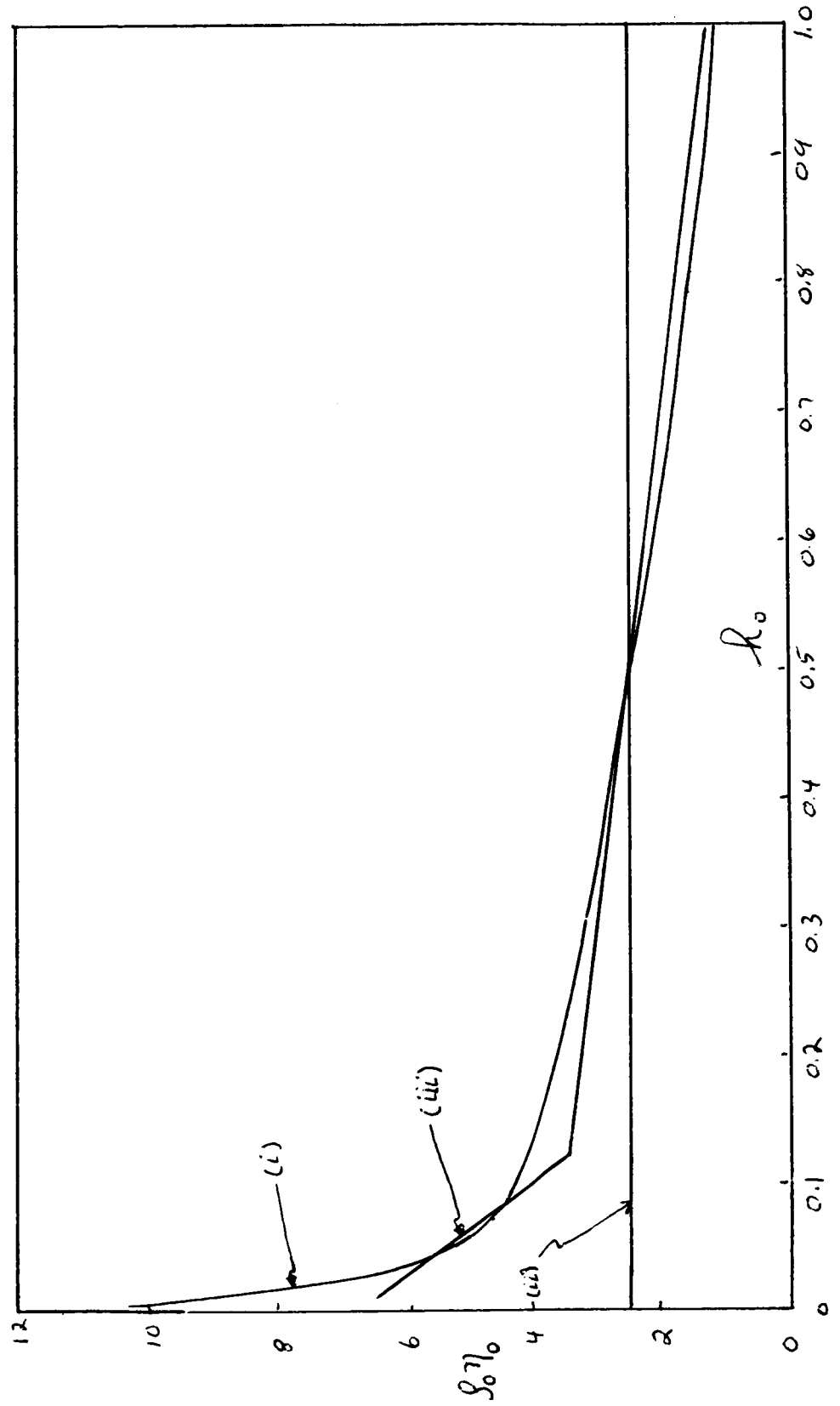

Fig. 9. Comparison of $\rho_o \eta_o$ valves:
(i) equilibrium air ($h^o = 8 \times 10^7$ J/Kg),
(ii) $\rho_o \eta_o = 2.5$ for analytic solution,
(iii) model gas for numerical solution.

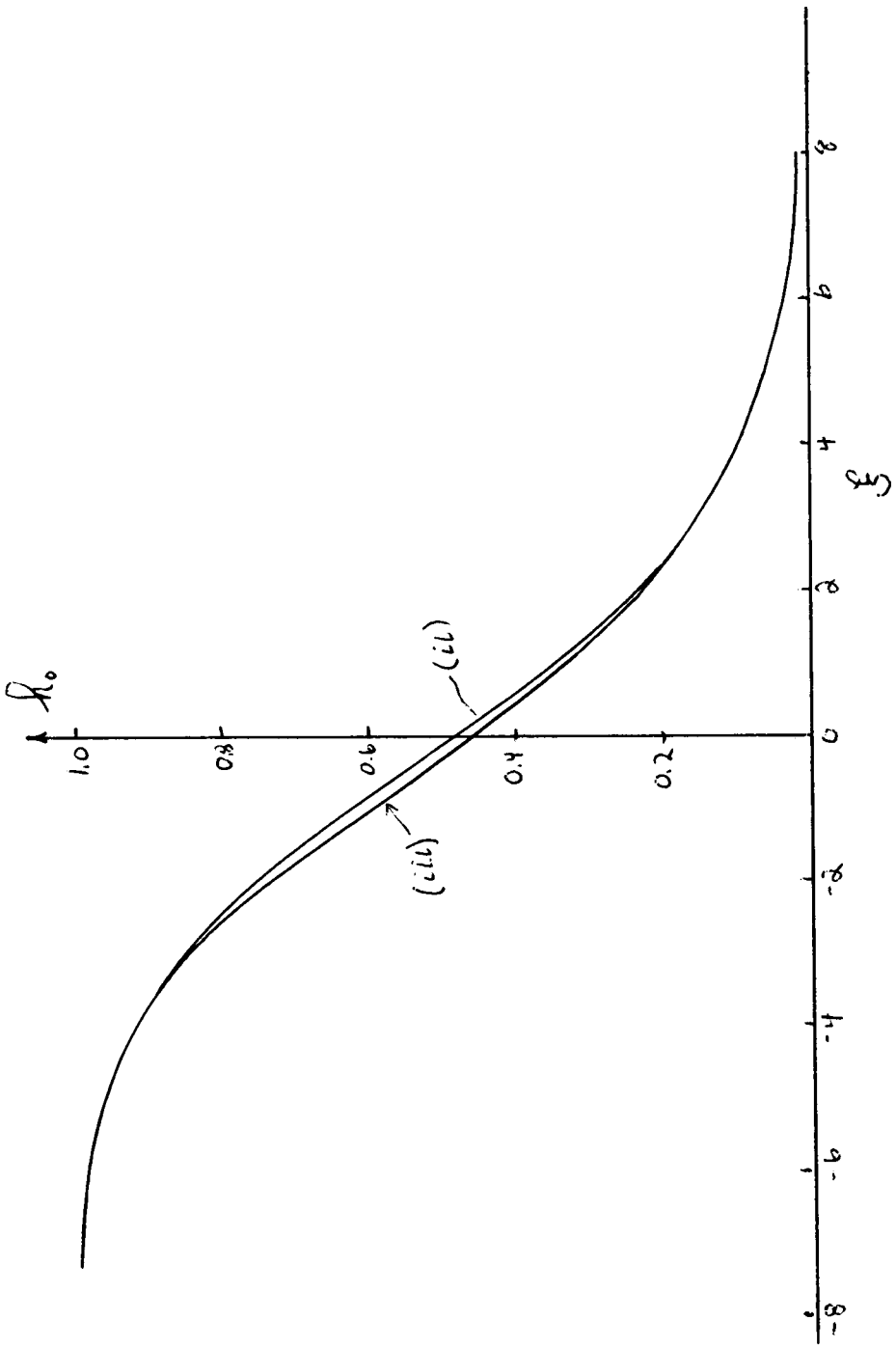

Fig. 10a. Enthalpy profile: (ii) analytic solution, (iii) numerical solution.

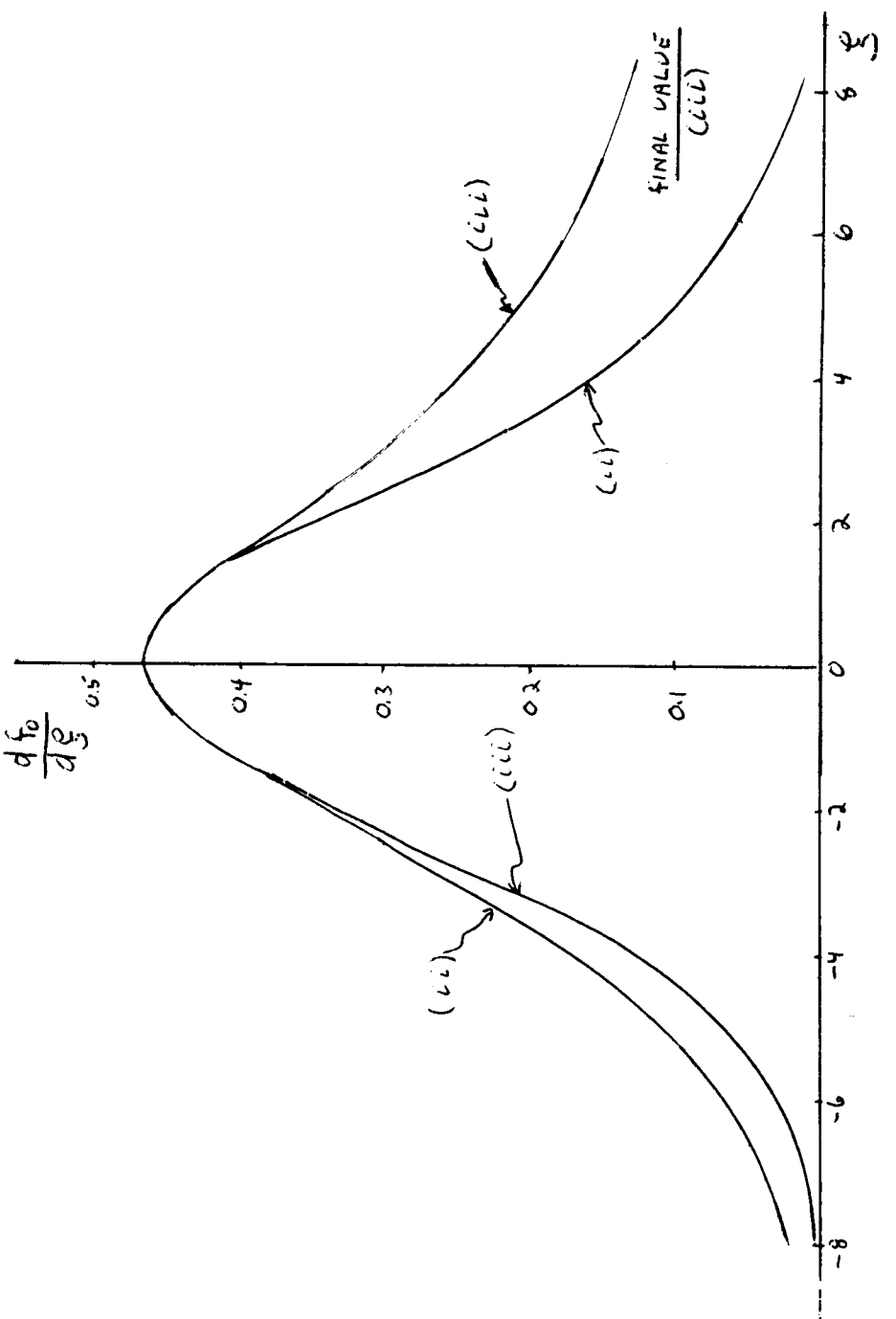

Fig. 10b. Velocity profile: (ii) analytic solution, (iii) numerical solution.

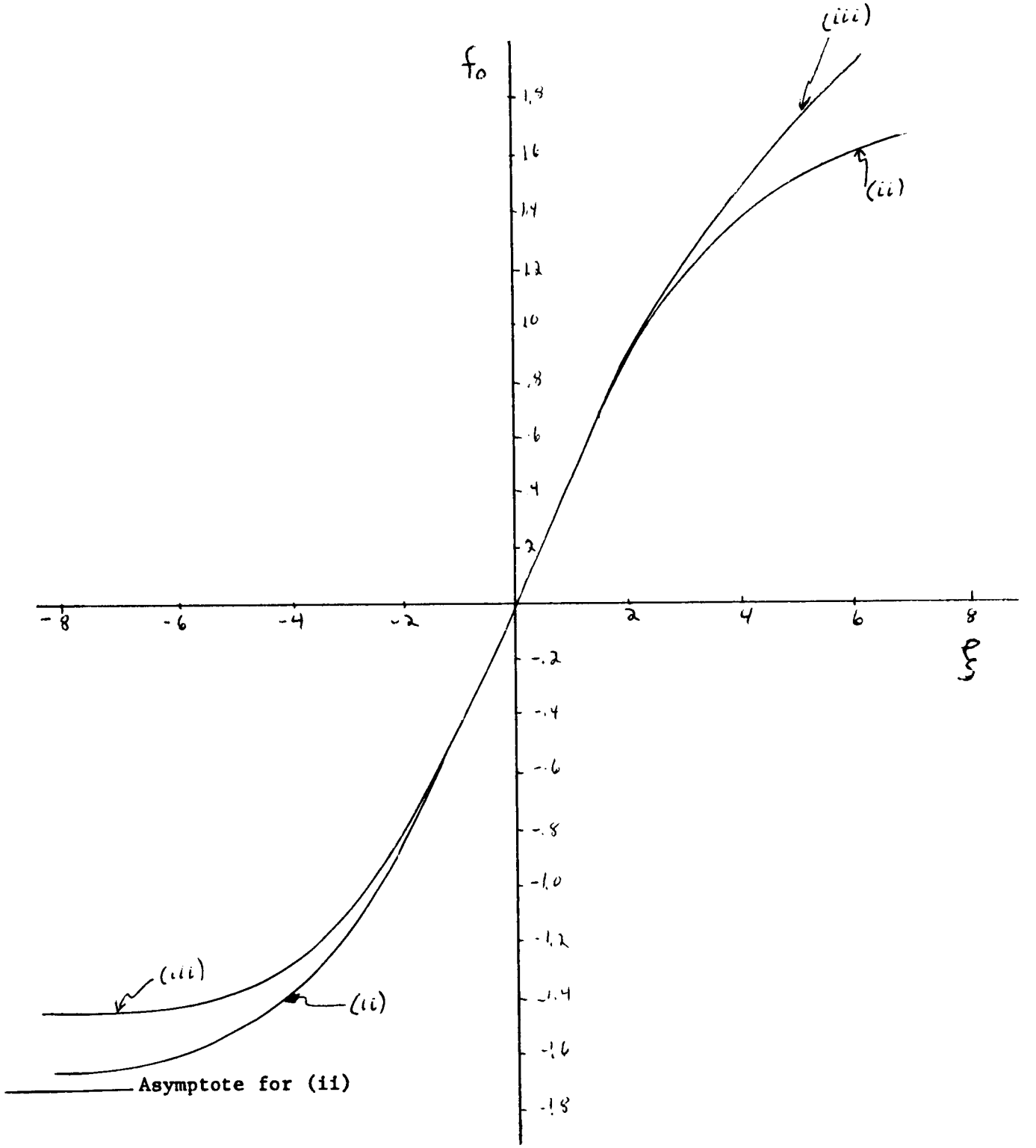

Fig. 10c. Transverse mass flow f_o:

(ii) analytic solution,
(iii) numerical solution.

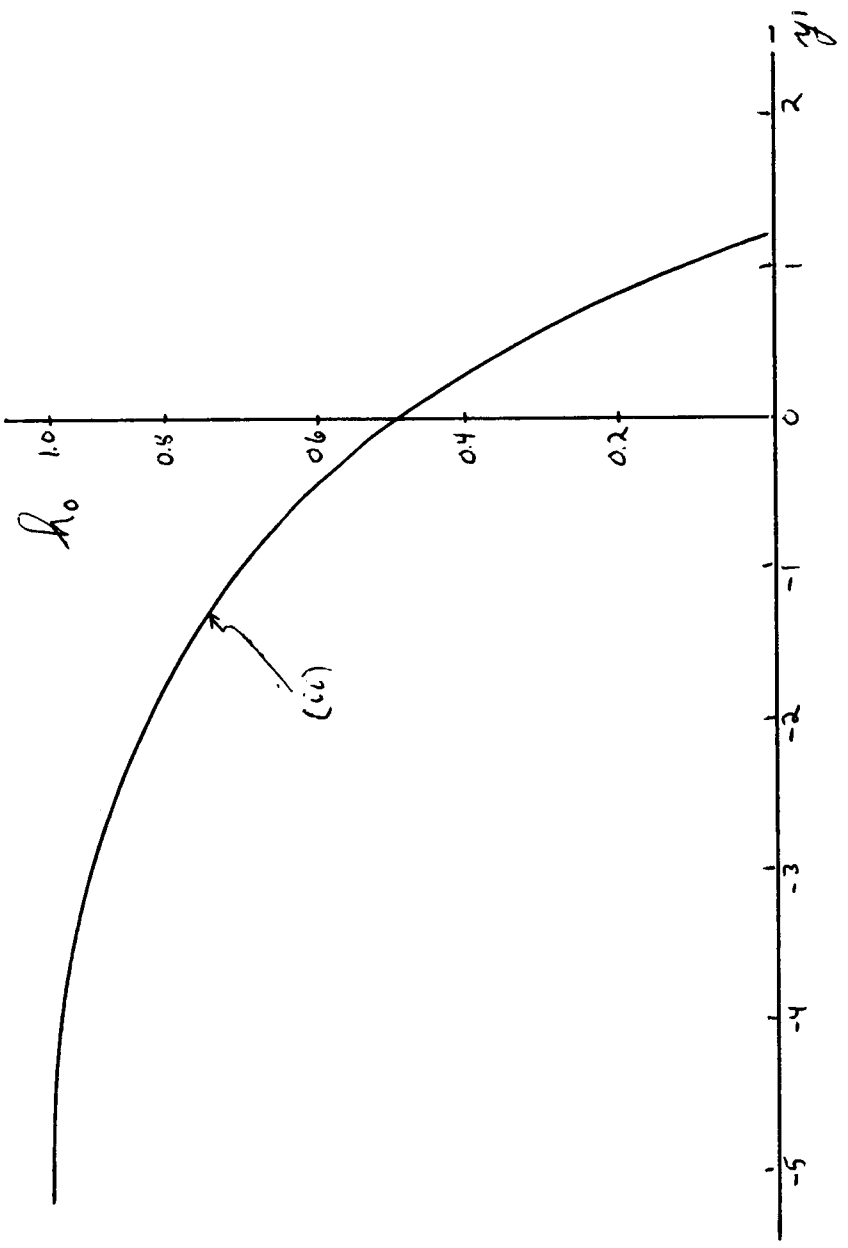

Fig. 11. Enthalpy profile in terms of physical coordinate y'

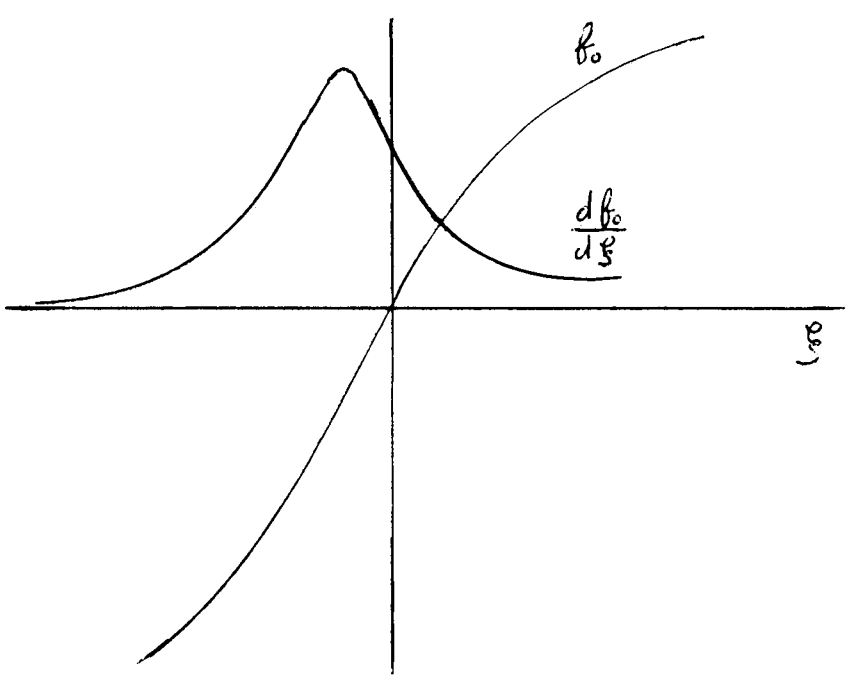

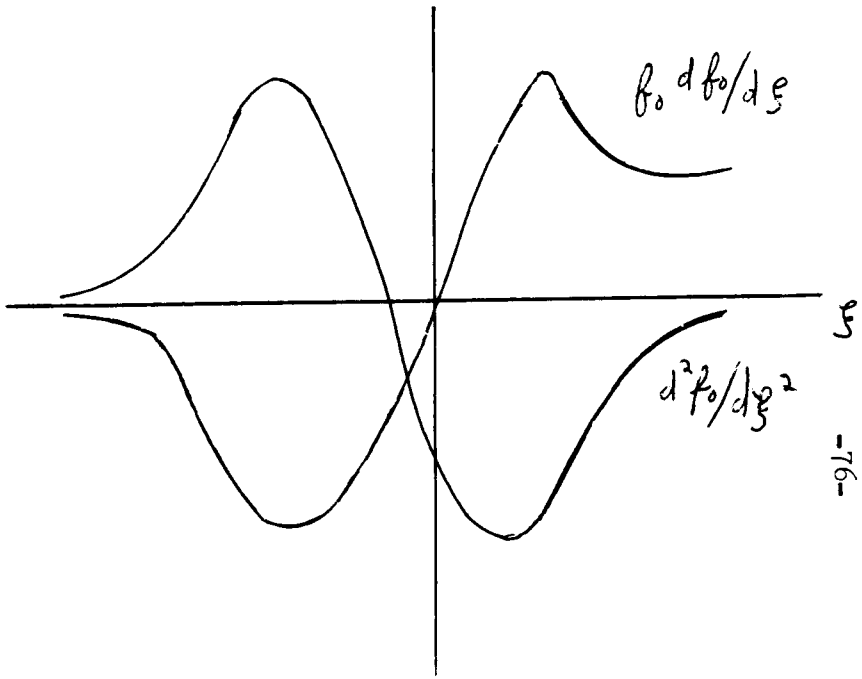

Fig. 12. Typical variation of $d^2f_o/d\xi^2$ and $f_o \, df_o/d\xi$

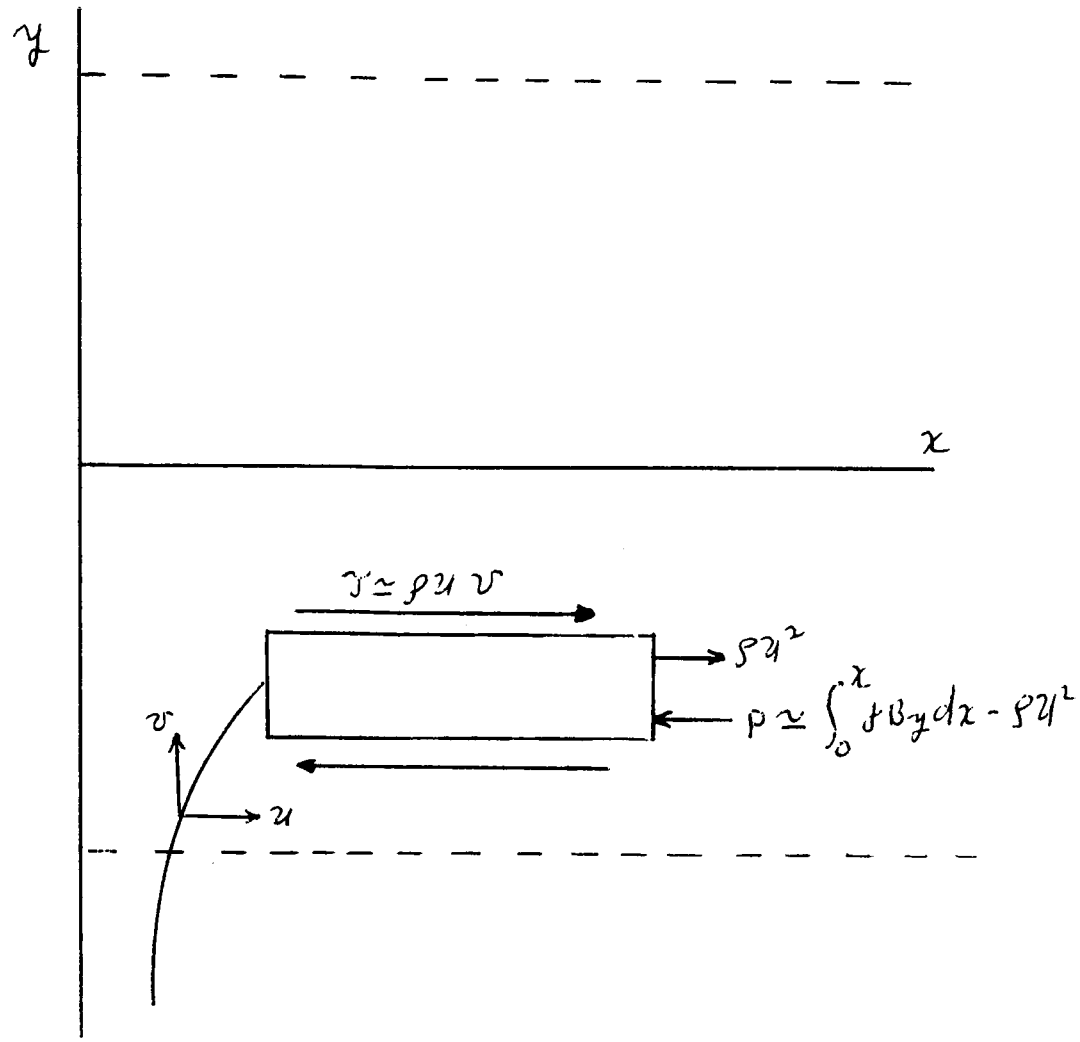

Fig. 13. Approximate force balance

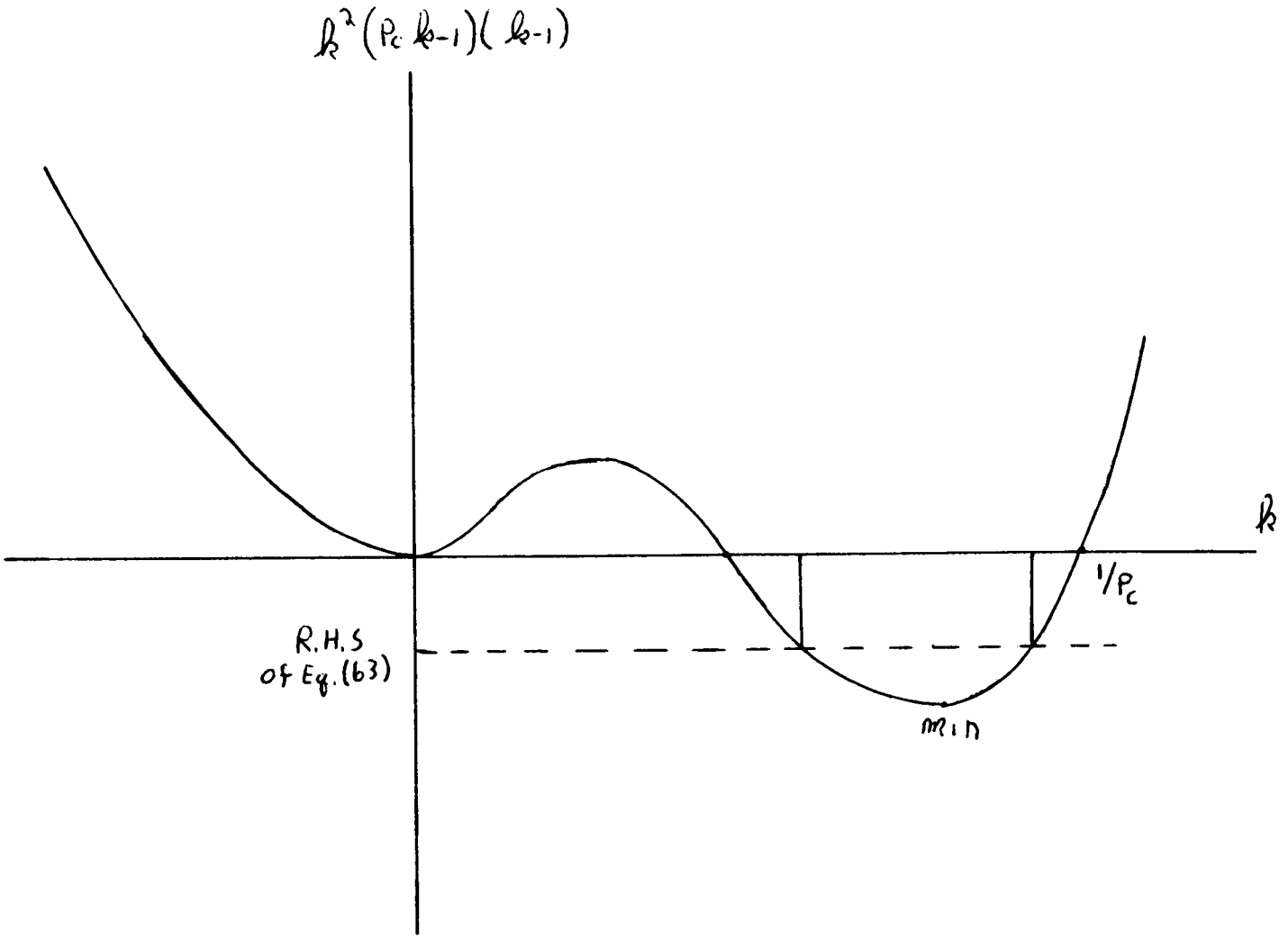

Fig. 14. Sketch of $k^2 (P_c k-1) (k - 1)$

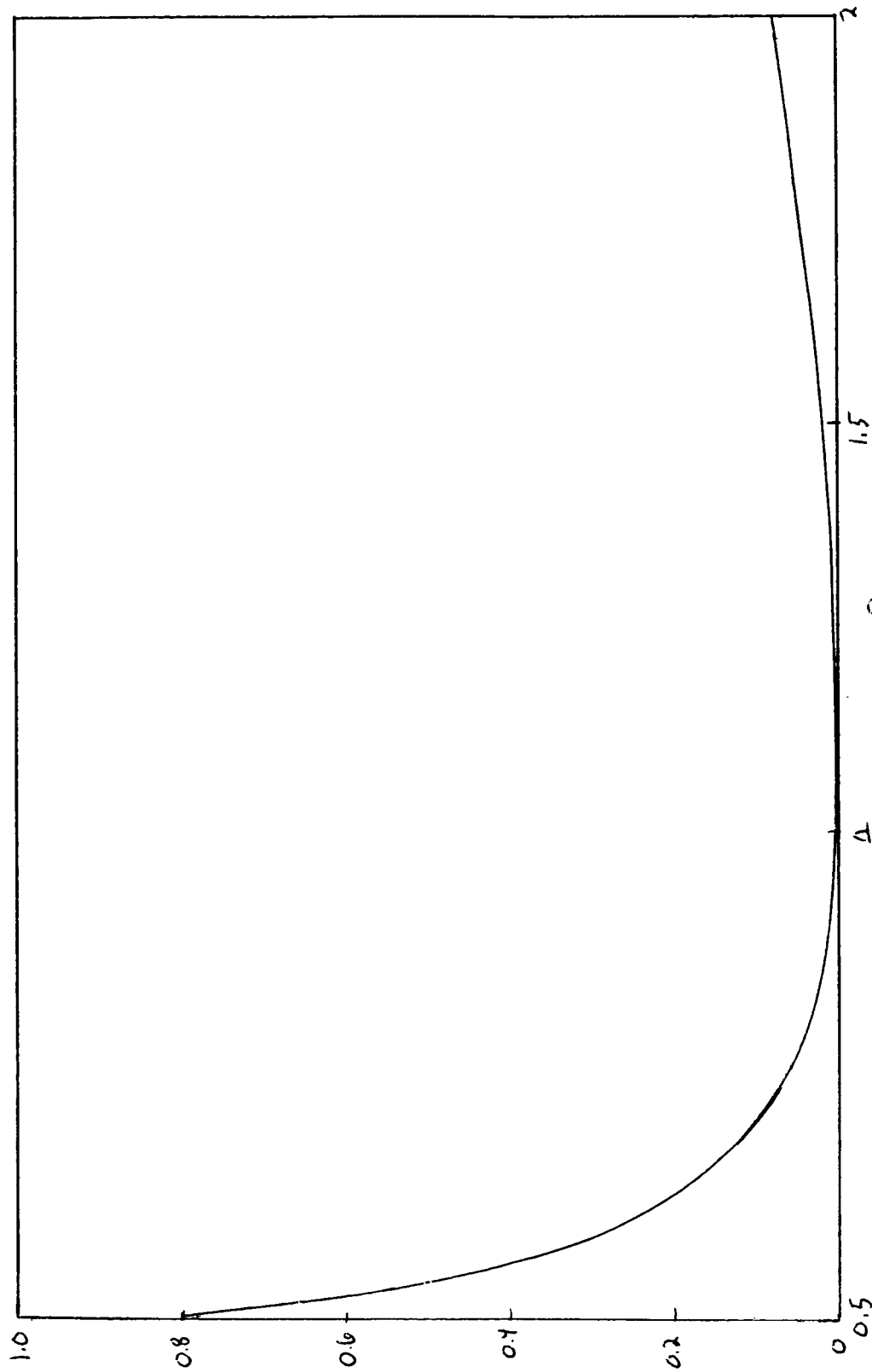

Fig. 15. Magnitude at the minimum of $k^2(P_c\ k-1)\ (k-1)^{P_c}$

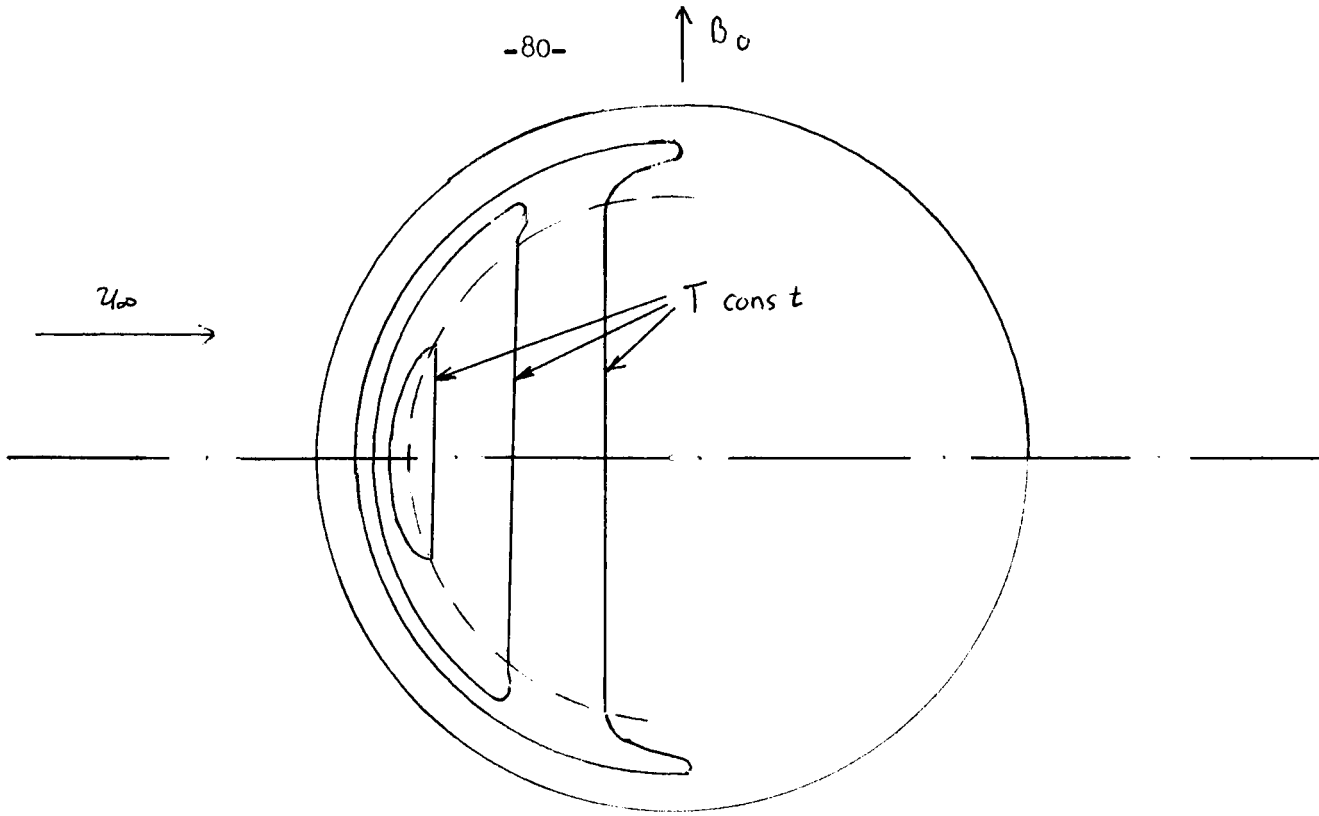

Fig. 16a. Possible isotherm pattern (field-line curvature neglected)

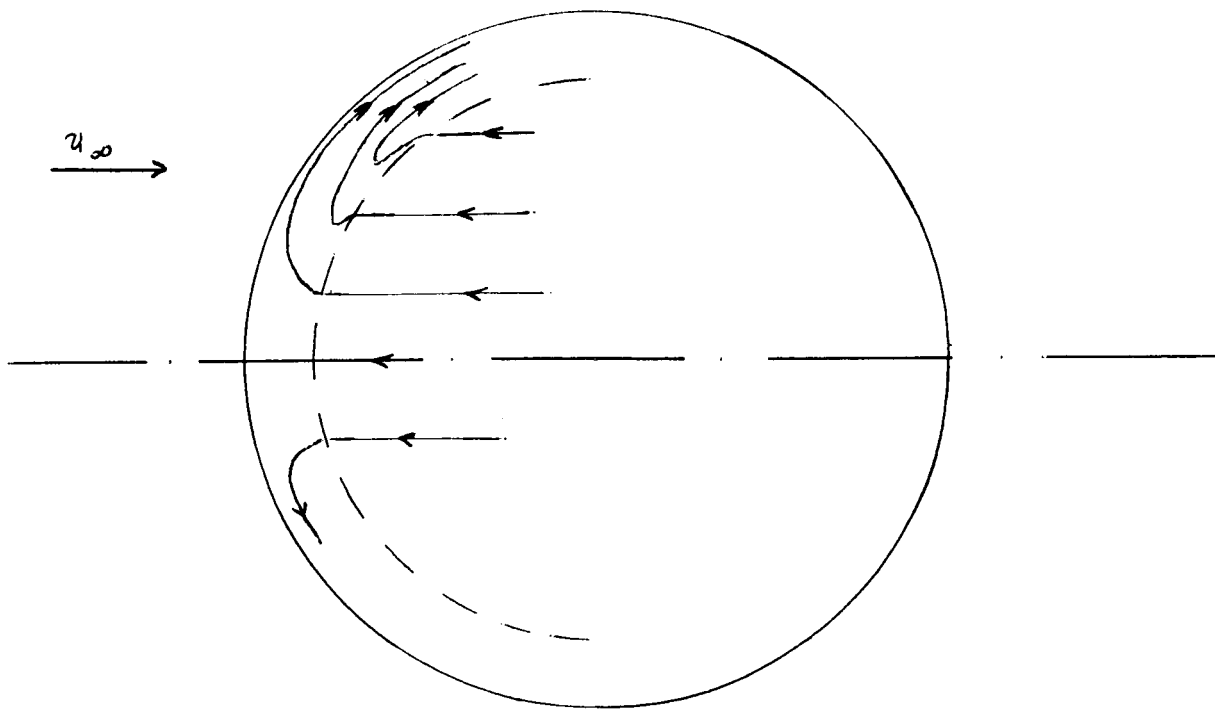

Fig. 16b. Possible streamlines, showing flow reversal

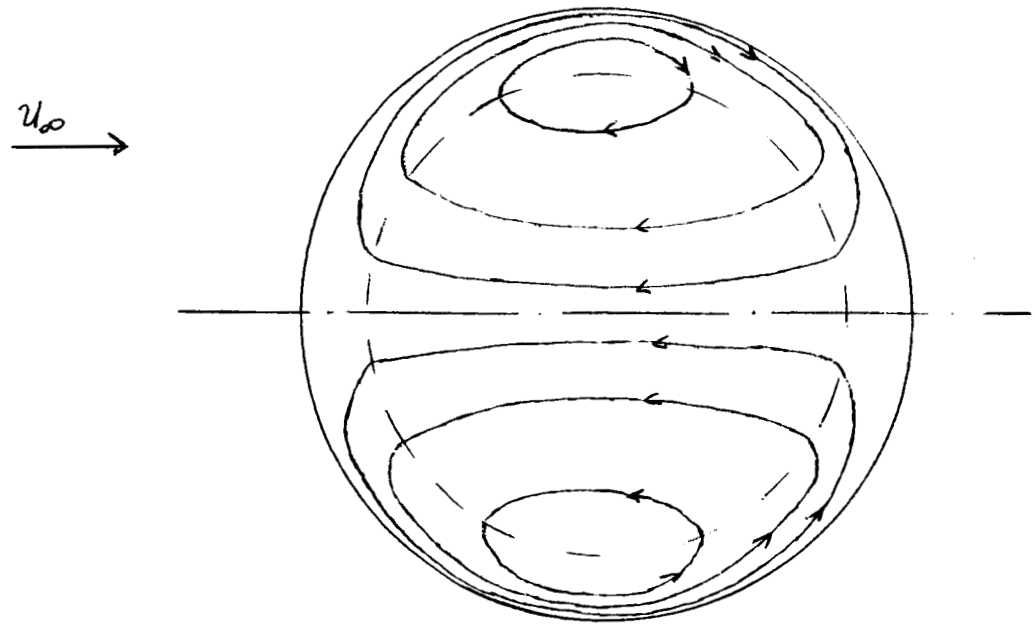

Fig. 17a. Possible streamline pattern for the Hall current

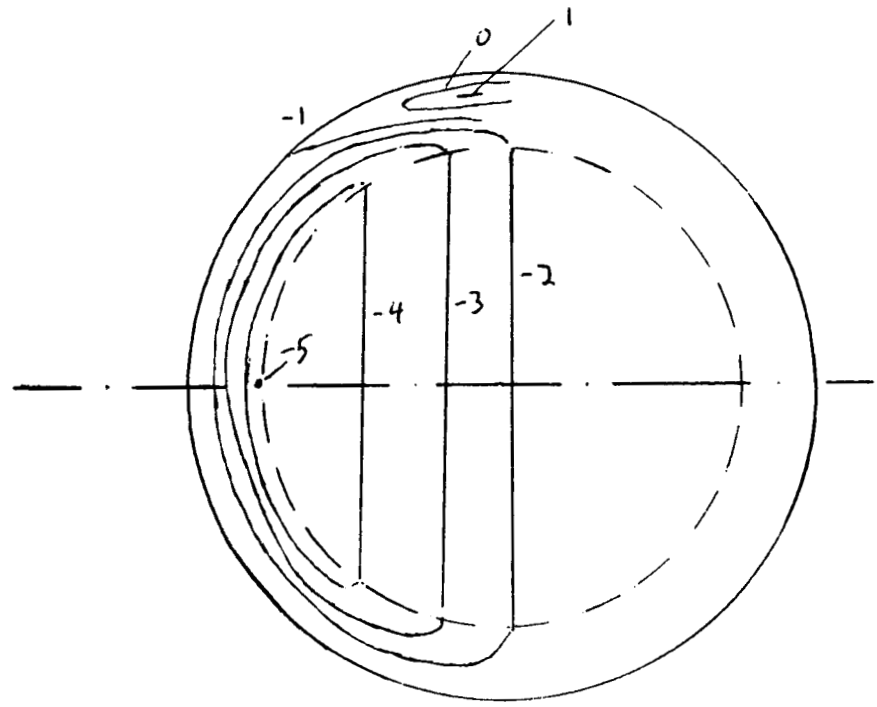

Fig. 17b. Possible form of V_H contours (arbitrary units)

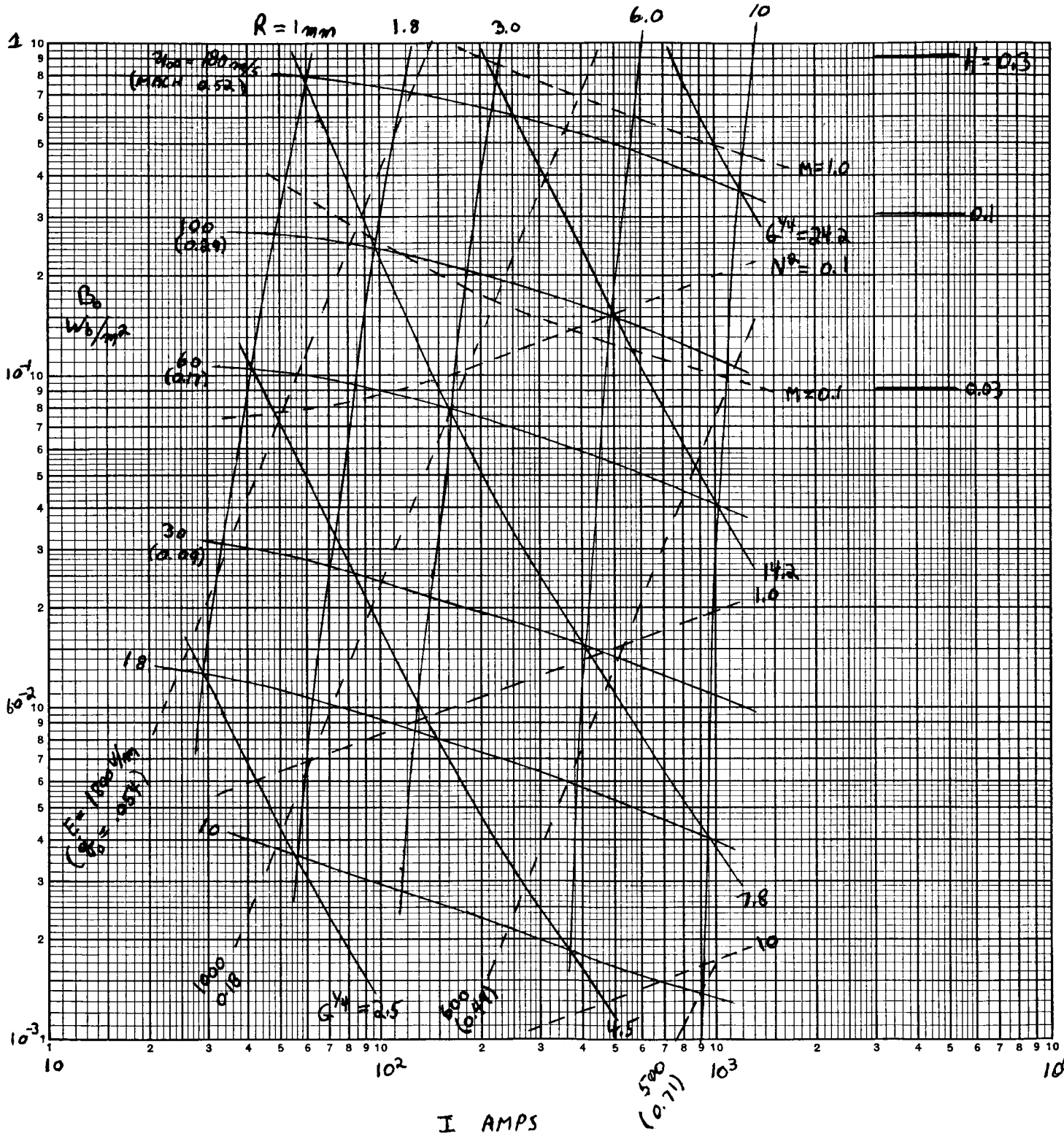

Fig. 18. Characteristic map for air at one atmosphere